



A study of a broadband balanced-bridge switching-state MOSFET mixer.

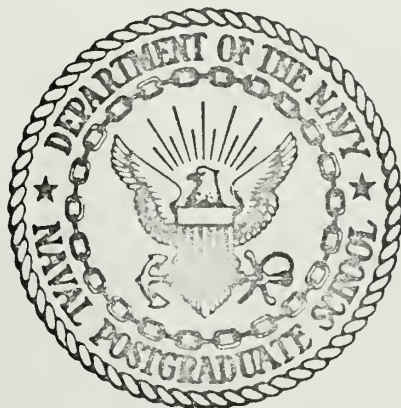
Title	A study of a broadband balanced-bridge switching-state MOSFET mixer.
Item Type	Thesis
Authors	Yenigün, Mustafa.
URI	https://hdl.handle.net/10945/15916
Date Issued	1971-12
Download date	2026-04-13 20:22:52
Link to Item	https://hdl.handle.net/10945/15916

Downloaded from NPS Archive: Calhoun

A STUDY OF A BROADBAND BALANCED-BRIDGE
SWITCHING-STATE MOSFET MIXER

Mustafa Yenigün

United States
Naval Postgraduate School



THE SIS

A STUDY OF A BROADBAND BALANCED-BRIDGE
SWITCHING-STATE MOSFET MIXER

by

Mustafa Yenigün

Thesis Advisor:

R. W. Adler

December 1971

T 1200

Approved for public release; distribution unlimited.

A Study of A Broadband Balanced-bridge
Switching-state MOSFET Mixer

by

Mustafa Yenigün
Lieutenant (junior grade), Turkish Navy
B.S., Naval Postgraduate School, 1971

Submitted in partial fulfillment of the
requirements for the degree of

MASTER OF SCIENCE IN ELECTRICAL ENGINEERING

from the
NAVAL POSTGRADUATE SCHOOL
December 1971

ABSTRACT

A theory for a mixer using four MOSFETs in a broadband balanced-bridge configuration has been developed in terms of both ideal models and approximate representations for departures from the ideal case. An interfering signal is assumed to be present in order to analyze intermodulation and cross-modulation distortions.

The mathematics of a MOSFET mixer are developed and compared with the conversion properties and intermodulation limitations of the simple nonlinear-resistance mixer.

Measurements are made in the 10-200 MHz range and close agreement with the theory is found for conversion loss. Disagreement in RF and LO isolations is attributed to stray capacitances and impedance mismatching. It is also shown that circuit-board and transformer design greatly affects performance of a mixer.

A comparison of MOSFET and hot-carrier diode double balanced mixers is given and it is indicated that the MOSFET mixer is superior in conversion loss and RF and LO isolations.

TABLE OF CONTENTS

I.	INTRODUCTION -----	8
II.	THEORETICAL ANALYSIS -----	15
	A. CONVERSION LOSS -----	18
	B. MIXER CHARACTERIZATION AND PARASITIC IMPEDANCE ANALYSIS -----	23
	C. INTERMODULATION DISTORTION -----	34
	D. SECOND HARMONIC TERMINATION -----	41
	E. DEVICE LIMITATIONS -----	41
	F. SUMMARY OF THEORETICAL ANALYSIS -----	44
III.	EXPERIMENTAL PROCEDURE -----	47
	A. MOSFETs -----	47
	B. TRANSFORMERS -----	47
	C. EXPERIMENTAL SET-UP, EXPERIMENTS AND LIMITATIONS -----	50
	D. RESULTS AND COMPARISON-----	55
IV.	CONCLUSIONS AND RECOMMENDATIONS -----	64
	APPENDIX A: A NONLINEAR RESISTANCE MIXER -----	67
	BIBLIOGRAPHY -----	74
	INITIAL DISTRIBUTION LIST -----	75
	FORM DD 1473 -----	76

LIST OF TABLES

I. Comparison of the Mixers ----- 62

LIST OF ILLUSTRATIONS

1.	I-V Plot of Ideal MOSFET -----	11
2.	Ideal Model of a MOSFET Balanced-bridge Switching-state Mixer -----	11
3.	Balanced-bridge Configuration of MOSFET Switching-state Mixer -----	14
4.	Gate Bias Network -----	16
5a.	Square-wave Reversing Function at LO Switching Rate -----	20
b.	Representation of Mixer as Three-port Linear Network -----	20
6.	"ON-state" Current Flows and Voltage Drops -----	24
7.	"ON-state" Voltage Drops Model -----	28
8.	"OFF-state" Current Flows and Voltage Drops -----	29
9.	State-1 Current Flows and Voltage Drops -----	30
10.	State-2 Current Flows and Voltage Drops -----	30
11.	"OFF-state" Current Flows Model -----	31
12.	The Total Mixer Characterization -----	32
13.	State-1 Equivalent Circuit with $Z_{ON} > 0$ and $Z_{OFF} = \infty$ -----	33
14.	Output Impedance Calculation -----	34
15.	Circuit for Varactor IM Calculation -----	40
16.	Usable Region of $I_D - V_{DS}$ Curve (Dotted Area) -----	43
17a.	LO Wave Form -----	45
b.	IM Because of Transition Time Behavior -----	45
18.	Transition Region -----	46
19.	Toroid Winding -----	49
20.	Schematic Showing the Connection of the Trifilar Windings -----	49

21.	Experimental Set-up -----	51
22.	LO Input Network -----	53
23.	IF Power Versus RF Power for $P_{LO} = 18$ dbm, $f_{RF} = 10-50$ MHz and $f_{LO} = 40-70$ MHz -----	56
24.	IF Power Versus RF Power for $P_{LO} = 25$ dbm, $f_{RF} = 75-150$ MHz and $f_{LO} = 105-180$ MHz -----	57
25.	Conversion Loss Versus LO Power for $P_{RF} = 0$ dbm, $f_{RF} = 12$ MHz and $f_{LO} = 42$ MHz -----	58
26.	Conversion Loss Versus LO Power for $P_{RF} = 0$ dbm, $f_{RF} = 23$ MHz and $f_{LO} = 53$ MHz -----	59
27.	Conversion Loss Versus LO Power for $P_{RF} = 0$ dbm, $f_{RF} = 40$ MHz and $f_{LO} = 70$ MHz -----	60
28.	Conversion Loss Versus LO Power for $P_{RF} = 0$ dbm, $f_{RF} = 75$ MHz and $f_{LO} = 105$ MHz -----	61
A-1.	Nonlinear Resistance Mixer -----	68

ACKNOWLEDGEMENT

The author wishes to express his appreciation to Professor R. W. Adler for the invaluable aid and counsel which he has offered during the preparation of this thesis.

I. INTRODUCTION

A mixer is a network containing one or more nonlinear devices which combines two unrelated signals to obtain a third signal at the sum or difference frequency. Mixers are extensively utilized in communication receivers, transmitters, radars and control systems.

Frequencies other than the sum and difference are also generated by the mixing action and they are called spurious responses. It will be shown that spurious responses generated by input and local oscillator signals are:

$$f_{IF} = \pm(nf_{LO} - mf_{RF}) \quad (I-1)$$

where

f_{IF} is the intermediate frequency (IF),

f_{LO} is the local oscillator (LO) frequency,

f_{RF} is the signal frequency (RF),

n, m are harmonic numbers of LO and RF frequencies, respectively.

The desired output of the mixer occurs when $m = n = 1$, such that:

$$f_{IF} = \pm(f_{LO} - f_{RF}) \quad (I-2)$$

In this case, one must note that the mixer will also respond to a signal at the image frequency (f_i), chosen such that:

$$f_i = f_{LO} + f_{IF} \quad (I-3)$$

and a signal at this frequency will combine with the LO signal to produce output at frequencies of the form $\pm f_i \pm f_{LO}$ and the difference product is also equal to the IF frequency. The normal procedure for eliminating the power at the image frequency at the input port of mixer will be described later in Section II.

Spurious responses occur at frequencies for which m or $n \neq 1$. These spurious responses can be reduced in number by means of selective circuits (filters) at the mixer output.

A large signal, f_1 , close to the signal frequency can interact with the signal to produce third-order intermodulation (IM) distortion at frequencies $2f_1 \pm f_{RF}$ and $2f_{RF} \pm f_1$. If f_{RF} and f_1 are arbitrarily close to one another the third-order IM signals are close to the input signal, f_{RF} , and will generate frequencies within the filter bandwidth at the mixer output.

The change in the amplitude of the interfering signal, f_1 , will also cross-modulate (CM) the output of mixer.

Spurious responses and IM distortions can be reduced or completely eliminated by careful mixer design. Therefore, mixer design becomes extremely important in high level signal environments in establishing receiver performance. There is a need to design mixers with the widest possible dynamic range and low conversion loss.

Non-linear devices typically employed by mixers are vacuum tubes, semiconductor diodes, bipolar transistors and FETs. In this study attention will be focused on an active broadband mixer using MOSFETs.

An insulated-gate MOSFET offers the advantages of extremely high input resistance, low input capacitance, very low feedback capacitance, high forward transconductance, and low noise at very high frequencies. Because of their insulated-gate construction these devices have extremely low leakage currents which are relatively insensitive to temperature variations. In addition, their drain currents have a negative temperature coefficient which makes "thermal runaway" virtually impossible. The high input resistance of MOSFETs permits the use of simple electron-tube type biasing techniques. It also makes these devices capable of handling relatively large positive and negative input signal excursions without degradation of input impedance due to diode current loading. Because of this capability, MOSFETs have considerably greater dynamic ranges than the other types of solid-state semi-conductor devices. In addition, MOSFETs exhibit electrical characteristics which result in low noise, CM, low IM distortion and high conversion efficiency.

The choice of MOSFETs for the experimental version in this balanced-bridge switching-state mixer was dictated by the unavoidable departures from ideal switching states. The device switching characteristic must occupy both the first and third quadrants of its I-V plot and the MOSFET has these regions of its normal operation that is shown in Figure 1; and the idealized model of a balanced-bridge switching-state mixer using MOSFETs as reversing switches is shown in Figure 2 (substrates were not shown for clarity).

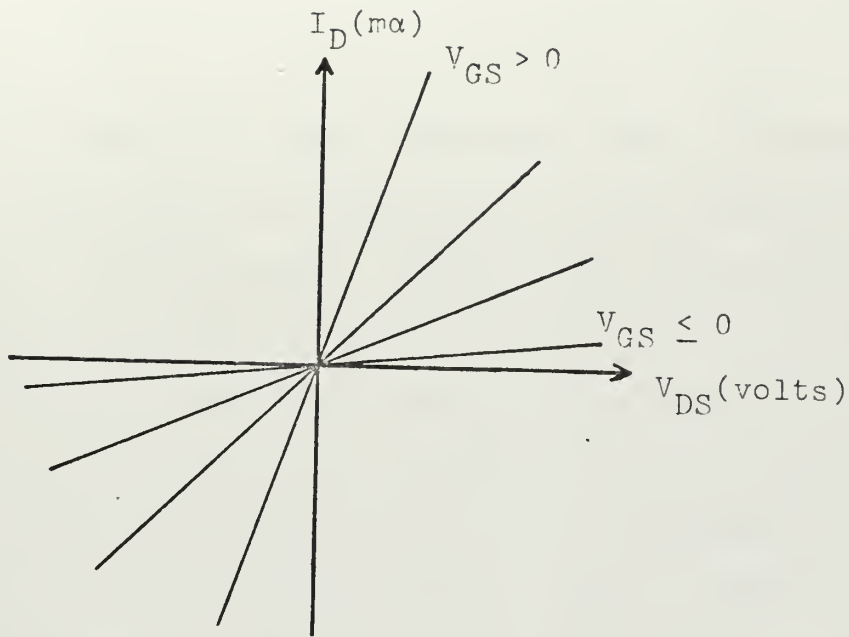


Figure 1. I-V Plot of Ideal MOSFET.

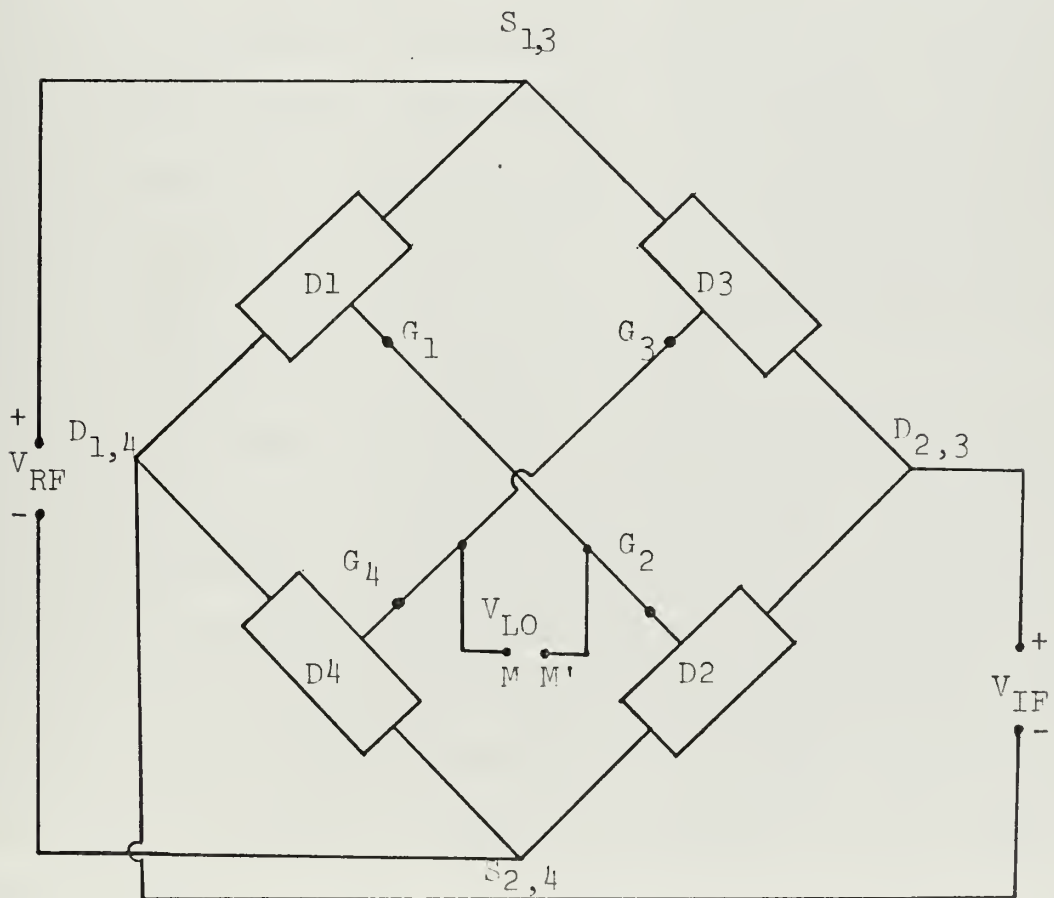


Figure 2. Ideal Model of a MOSFET Balanced-bridge Switching-state Mixer.

A double-balanced mixer allows energy to be exchanged on a full-wave cycle rather than half cycle, therefore, offers higher efficiency and lower conversion loss. Spurious responses generated by the harmonics of the signal and LO frequencies are eliminated. Ideally the conversion loss of a balanced-bridge switching-state mixer is zero and the output contains no third-order spurious responses, which are one of the most troublesome distortion terms in mixers.

Layout becomes extremely important, especially at high frequencies. Nearly perfect balance can be obtained by symmetrical layout and using careful VHF construction techniques, i.e., short leads and short ground returns. Wide bandwidth is obtained by designing toroidal transformers with tight coupling between the windings and carefully choosing the core materials. The self-shielding feature of toroidal transformers makes it possible to mount toroids against a printed-circuit (PC) board, a metal chassis or cabinet wall, without significantly affecting their Q.

Balanced-bridge MOSFET mixers require relatively high LO injection power for lowest conversion loss. Most of the currently available literature on FET mixers is based on analysis in the square-law region only. Subsequently, validity is limited to low conversion gain operation. For high LO injection level operation, i.e., high conversion gain, there is little information available on the design of MOSFET mixers.

This mixer has a number of operational advantages: High port-to-port isolation (similar to carrier suppression in a

balanced modulator), wide dynamic range, low IM and CM, and good noise-figure.

A theoretical analysis is given in Section II for the mixer shown in Figure 3. The circuit was designed and tested within the 10-200 MHz range in order to verify the theoretical results.

IM products were not measured because the available spectrum analyser, signal generators and power amplifier produced so many spurious responses within themselves, it was virtually impossible to observe outputs of the circuit under test.

CM distortion was not demonstrated either because the low level output of the signal generators did not produce CM terms of sufficient amplitude for oscilloscope viewing.

A comparison of the theoretical and experimental results for the balanced-bridge switching-state MOSFET and a hot-carrier diode double-balanced mixers is given in Table I in Section III.

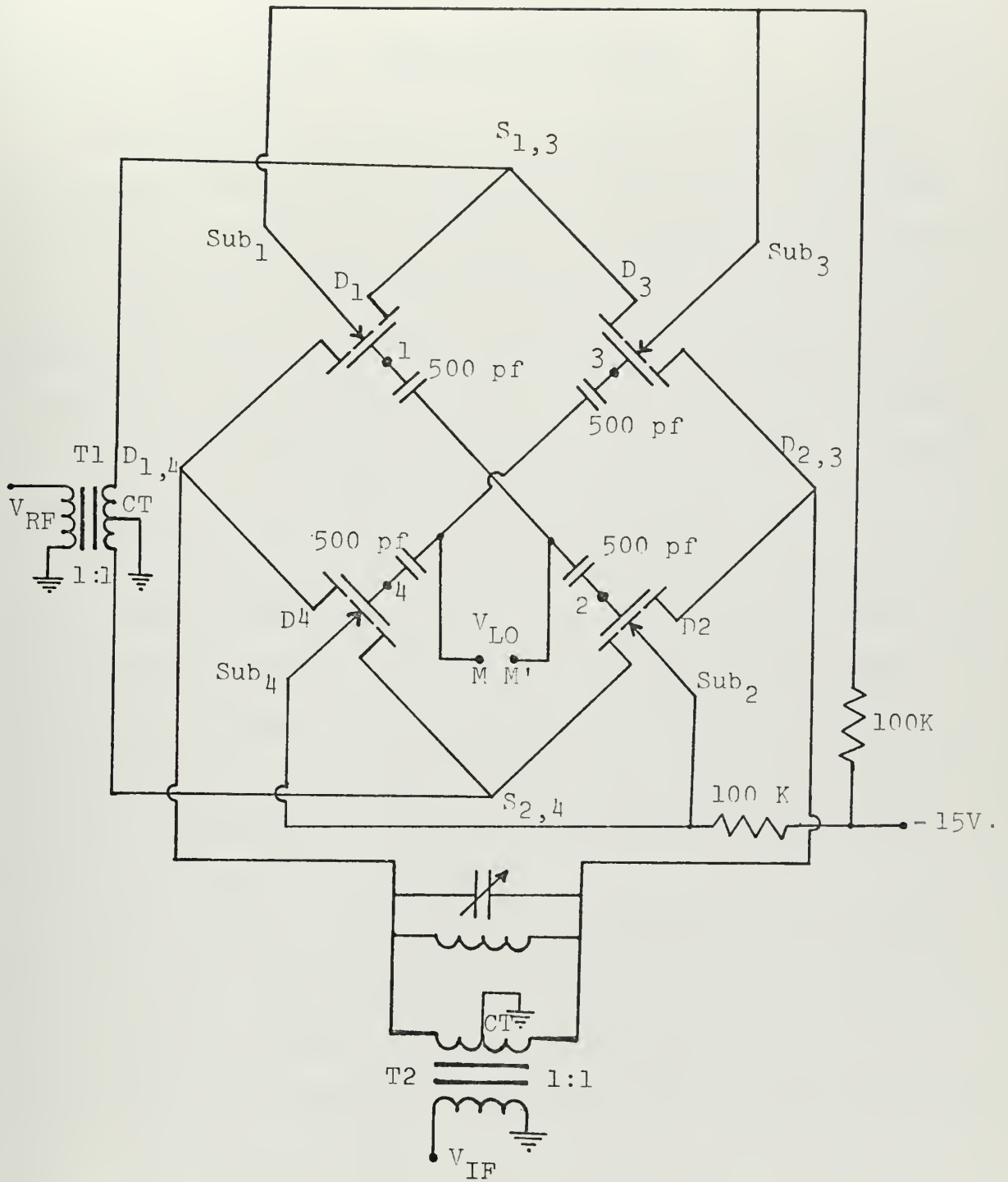


Figure 3. Balanced-bridge Configuration of MOSFET Switching-state Mixer.

II. THEORETICAL ANALYSIS

The objective of a mixer is to change the frequency of an incoming signal with maximum efficiency at the same time introducing minimum CM, IM distortion and noise. For mixers with a square-law transfer characteristic, both CM and IM distortion effects will be zero provided the range of the square-law is not exceeded by the LO amplitude. A convenient measure of the conversion efficiency is the conversion transconductance. This expresses the output current at the converted IF frequency in terms of the input signal amplitude. However, by itself this is not sufficient to ensure a high conversion gain. In addition the mixer output admittance must be small. The conversion transconductance of MOSFETs can be derived for the particular case of a square-law device in which the applied signals do not exceed the range over which the law applies.

In the following analysis, the performance of the mixer is given. An interfering signal is assumed to be present. A good understanding of the spurious responses, IM and CM distortions are necessary. Therefore, the following definitions are given.

"Spurious responses" occur at $\pm(nf_{LO} - mf_{RF})$ for n or $m \neq 1$ and can be reduced by biasing or mixer design. A gate bias network is included in the analysis as indicated in Figure 4.

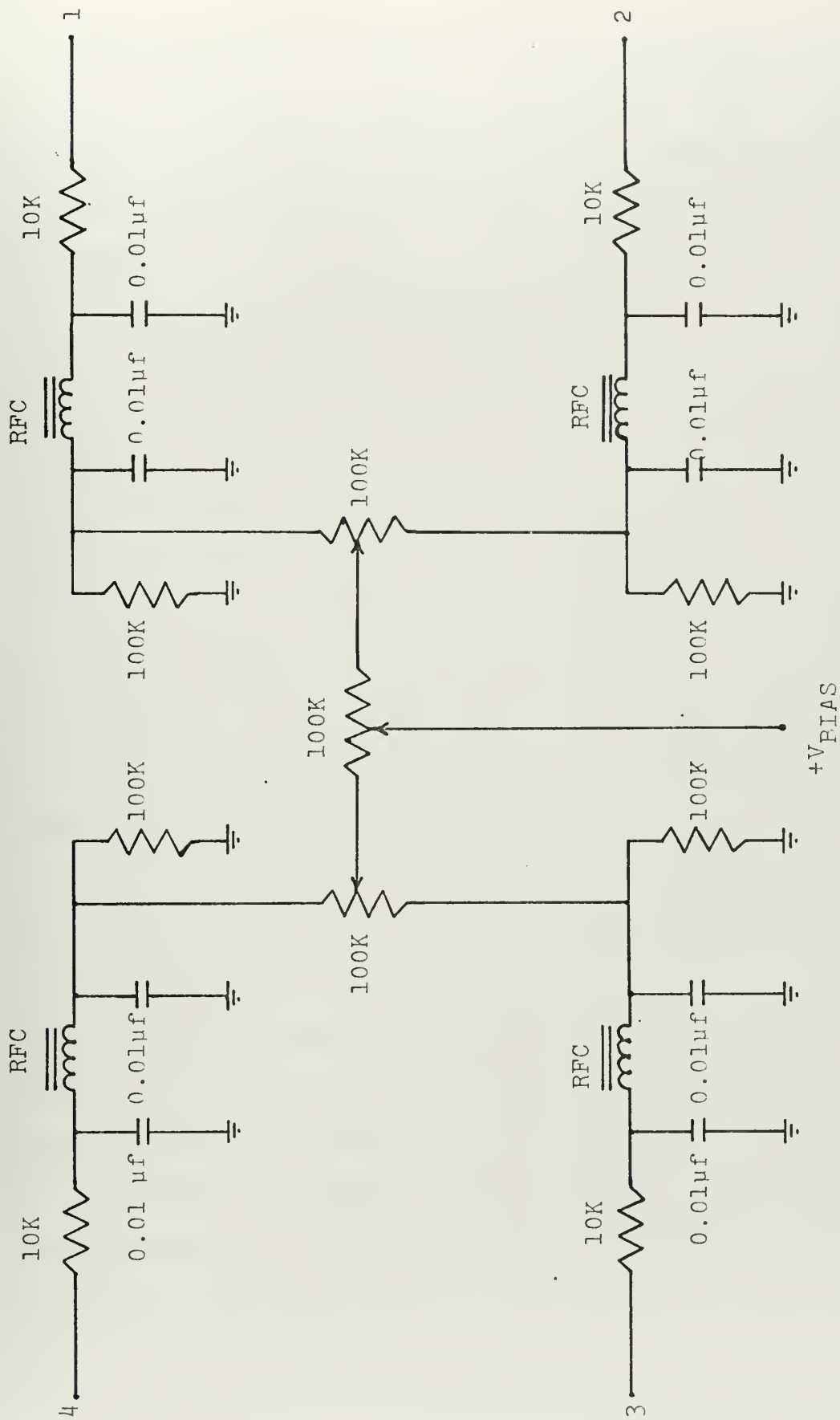


Figure 4. Gate Bias Network.

"IM responses" are formed when the mixer is subjected to one or more undesired signals. Two or more signals and the LO signal can mix and produce IM responses at frequencies which are represented by any linear combination of the input frequencies:

$$f_{IF} = \pm(nf_{LO} - kf_1 - qf_2 - mf_{RF}) . \quad (II-1)$$

Equation (II-1) accounts for IM responses in the mixer stage. Two undesired signals can mix and generate the desired signal due to the nonlinearities in the previous stages. This is also called IM response and named "receiver IM."

"CM response" occurs when the modulation on an undesired signal is transferred to a desired signal. CM is only modulation transfer rather than the frequency translation.

IM and CM distortions can not be eliminated by mixer design but IM responses can be reduced.

The simplest mixer is a nonlinear resistance together with proper frequency-dependent networks. This mixer version is described in the Appendix A.

Although the mixer used in this thesis is quite different in principle of operation, the fundamental limitations on its dynamic range and conversion loss can be estimated by modeling its departures from the ideal model as parasitic nonlinear resistances. In this study, the analysis is based upon mixer conversion loss.

A. CONVERSION LOSS

Ideally the mixer has zero conversion loss and RF input signal power is equal to IF output power such that $P_{RF} = P_{IF}$.

The method of operation of the balanced-bridge switching-state mixer is fundamentally different from the nonlinear-resistance method of frequency conversion. In its simplest form, it requires four devices with measurably different "ON" and "OFF" states, with a means for externally switching between the two states, that is shown in Figure 2. Opposite pairs of devices on the bridge are turned "ON" and "OFF" at the LO frequency, and the entire mixer may be modeled as a double-pole double-throw reversing switch changing state at the LO rate. The exact type of device is not important; in the ideal case they can be diodes, transistors, FETs or other two-state devices. In the ideal-model case, the transfer characteristics of the individual devices are unimportant. The choice of MOSFETs for the experimental version of this mixer was dictated by the unavoidable departures from ideal switching states, in which case the device characteristics are important. The individual devices may switch either voltage or current; the bridge configuration satisfies power conservation at either port.

As an illustration, assume devices D_1 and D_2 , D_3 and D_4 are paired two state current-control devices, controlled by the third terminal in the center of the bridge shown in Figure 2. Then, with D_1 and D_2 "OFF" (passing zero current) and D_3 and D_4 "ON," $I_{out} = I_{in}$ and $V_{out} = V_{in}$; with D_1 and

D_2 "ON," and D_3 and D_4 "OFF," $I_{out} = -I_{in}$ and $V_{out} = -V_{in}$, the ideal model is a reversing switch. If the switch poles are driven at some switching rate $E(T)$, where $E(T)$ is a square-wave reversing function, shown in Figure 5a, such that:

$$E(T) = \frac{2}{\pi} \sum_{n=\pm \text{ odd}}^{\infty} \frac{e^{j2\pi f_{LO}nt}}{|n|} (-1)^{(|n|-1)/2}, \quad (\text{II-2})$$

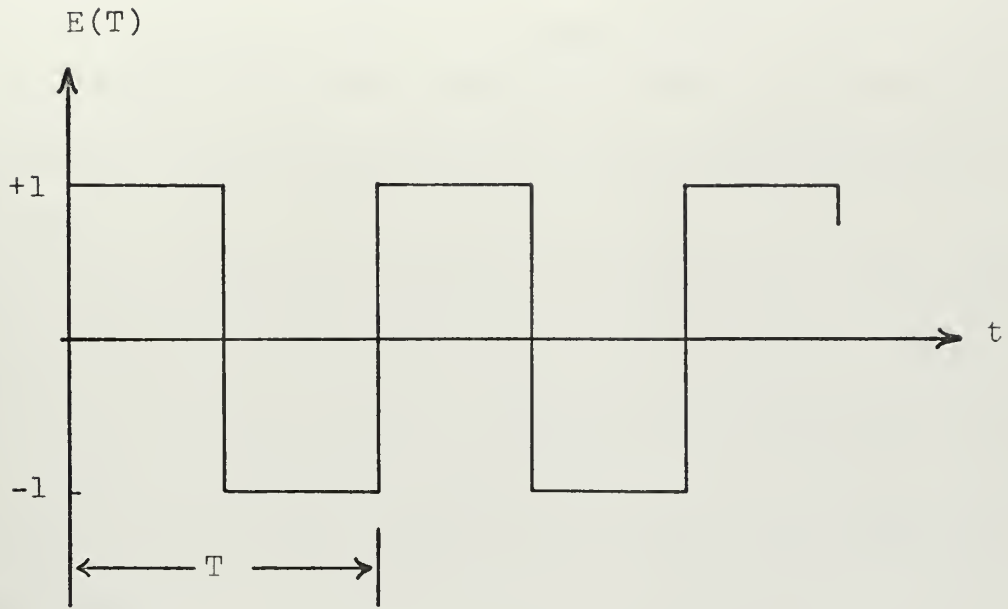
it is then possible to define a LO frequency $\omega_{LO} = \frac{2\pi}{T}$. If $V_{in} = V_{RF} \cos \omega_{RF} t$, then $V_{out} = V_{in} E(T)$ and,

$$V_{out} = V_{RF} \frac{2}{\pi} [\cos(\omega_{LO} + \omega_{RF})t + \cos(\omega_{LO} - \omega_{RF})t] \\ + \text{Higher Order Terms.} \quad (\text{II-3})$$

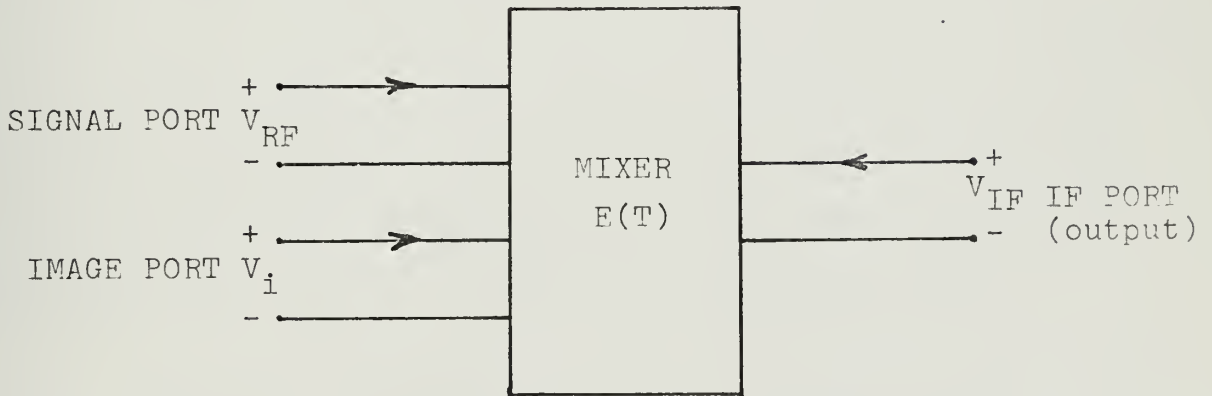
The higher order terms are all odd-order, of the form $n\omega_{LO} \pm \omega_{RF}$ where n is odd.

It should be noted at this point that frequency conversion has been achieved with nothing said about nonlinear resistance or individual device characteristics at all; the only assumption made was that both perfect switched states are attainable. For non-perfect switching the situation is more complicated, as will presently be shown. For the moment, attention will be concentrated on evaluating the output signals and the effects of frequency dependent terminations.

Assuming a square-wave switching wave form, the mixer can be modeled as a three-port network shown in Figure 5b, not unlike the conventional mixer. The difference is that the black box has a simple time domain operation $E(T)$, corresponding to the frequency domain operation of mixing. At the



(a). Square Wave Reversing Function at LO Switching Rate.



(b). Representation of Mixer as Three-port Linear Network.

Figure 5.

IF output port, $V_{IF} = V_{RF}E(T)$ and $I_{IF} = I_{RF}E(T)$. Since $E(T)E(T) = 1$, $V_{RF} = V_{IF}E(T)$ and $I_{RF} = I_{IF}E(T)$ and the mixer is bi-lateral in that the output and the input ports can be interchanged without affecting the conversion properties of the mixer.

Assuming a desired signal at RF frequency is the only signal available at the input port, the output voltage is,

$$V_{out} = \frac{2}{\pi} V_{RF} \left[\cos(\omega_{LO} - \omega_{RF})t + \cos(\omega_{LO} + \omega_{RF})t \right]. \quad (II-4)$$

The output voltage has components at both the IF and sum frequencies,

$$V_{out} = \frac{2}{\pi} \left[V_{RF} + V_{sum} \right]. \quad (II-5)$$

It is possible to eliminate the sum frequency power at the output with a parallel-tuned LC trap set at the IF frequency; this sets $V_{sum} = 0$ at the output, and

$$V_{out} = V_{IF} = \frac{2}{\pi} V_{RF}. \quad (II-6)$$

Since the mixer is completely bi-lateral the IF voltage can be considered as an input signal at the reverse input port.

Then $V'_{RF} = V_{IF}$ and the voltage at the input port is,

$$V_{reverse} = \frac{2}{\pi} V_{IF} \left[\cos(\omega_{LO} + \omega_{IF})t + \cos(\omega_{LO} - \omega_{IF})t \right]. \quad (II-7)$$

This has components at the signal and the image frequencies,

$V_{RF(reverse)} = \frac{2}{\pi} V_{IF}$ and $V_{i(reverse)} = \frac{2}{\pi} V_{IF}$. Hence,

$$V_{IF} = \frac{\pi}{2} V_{RF(reverse)} = \frac{\pi}{2} V_{i(reverse)}. \quad (II-8)$$

It is clear from Equation (II-8) that if the input appears as a short circuit at the image frequency, the IF output voltage drops to zero. The normal method of separating the signal and image ports and eliminating image response is to short circuit the image frequencies at the input; this is clearly impossible here.

A similar analysis, performed for the current frequency components, shows that it is possible to terminate the currents independently of the voltages. The image frequency power may be eliminated at the input by open circuiting the input at the image frequency; the $I_{i(\text{forward})}$ becomes zero and the image frequency power, P_i , also becomes zero. Thus the image response may be eliminated by allowing no image frequency current to flow at the input, and sum frequency power by short circuiting the output for all but the IF frequency. Reversal of the input or output constraint (open circuiting the sum at the output instead of short circuiting it) requires reversing the other constraint. To summarize,

1. If the sum frequency is shorted at the output, then the image frequency must be open circuited at the input, or
2. If the sum frequency is open circuited at the output, then the image frequency must be shorted at the input.

The above equations show that shorting the signal frequency voltage or open circuiting its current will eliminate the IF frequency voltage or current at the output, which is not particularly surprising. Under short circuit sum, open

circuit image constraints, the input impedance for some load resistance, R_L , will be $\frac{4}{\pi^2} R_L$; the output current is $\frac{2}{\pi}$ times the signal current, since the apparent constraints are reversed for current (with the constraints reversed for voltage, the input impedance is $\frac{\pi^2}{4} R_L$). The total output power is,

$$P_{IF} = \frac{\pi}{2} V_{RF} \frac{2}{\pi} I_{RF} = P_{RF} , \quad (II-9)$$

and the mixer conversion loss is zero.

It is clear that the conversion loss of the mixer with parasitic impedances will be greater than zero, since the real parts of the "ON" and "OFF" device impedance represent dissipated power as a device limitation. For this reason conversion loss is described again at the end of II-B.

B. MIXER CHARACTERIZATION AND PARASITIC IMPEDANCE ANALYSIS

The mixer characterization, in this thesis, is based upon parasitic impedances. The following analysis will be a first attempt to describe the effects of the parasitic impedances. The mixer will first be analyzed under the assumption that the "OFF-state" of the devices is perfect (no reverse current) and that there is a small but measurable voltage drop across the "ON" devices. The assumptions are then reversed, with the effects of "OFF-state" current flow analyzed, with the voltage across the "ON" devices equal to zero. These approximate solutions should be sufficient for estimates of the conversion loss and IM generation levels of the mixer (though a slightly different approach is more

rewarding in the investigation of conversion loss). A simple extension of the analysis will allow an iterative solution.

It is worthwhile to separate the "common-mode" and "difference-mode" voltages and currents as measured on the terminals of the mixer as indicated in Figures 6 and 8. In addition, the parasitic impedances are separated into odd-order and even-order terms, with the parasitic voltages or currents also divided into odd and even order components.

For Figure 6, the mixer will be analyzed in terms of total voltage drops around the input and output paths for

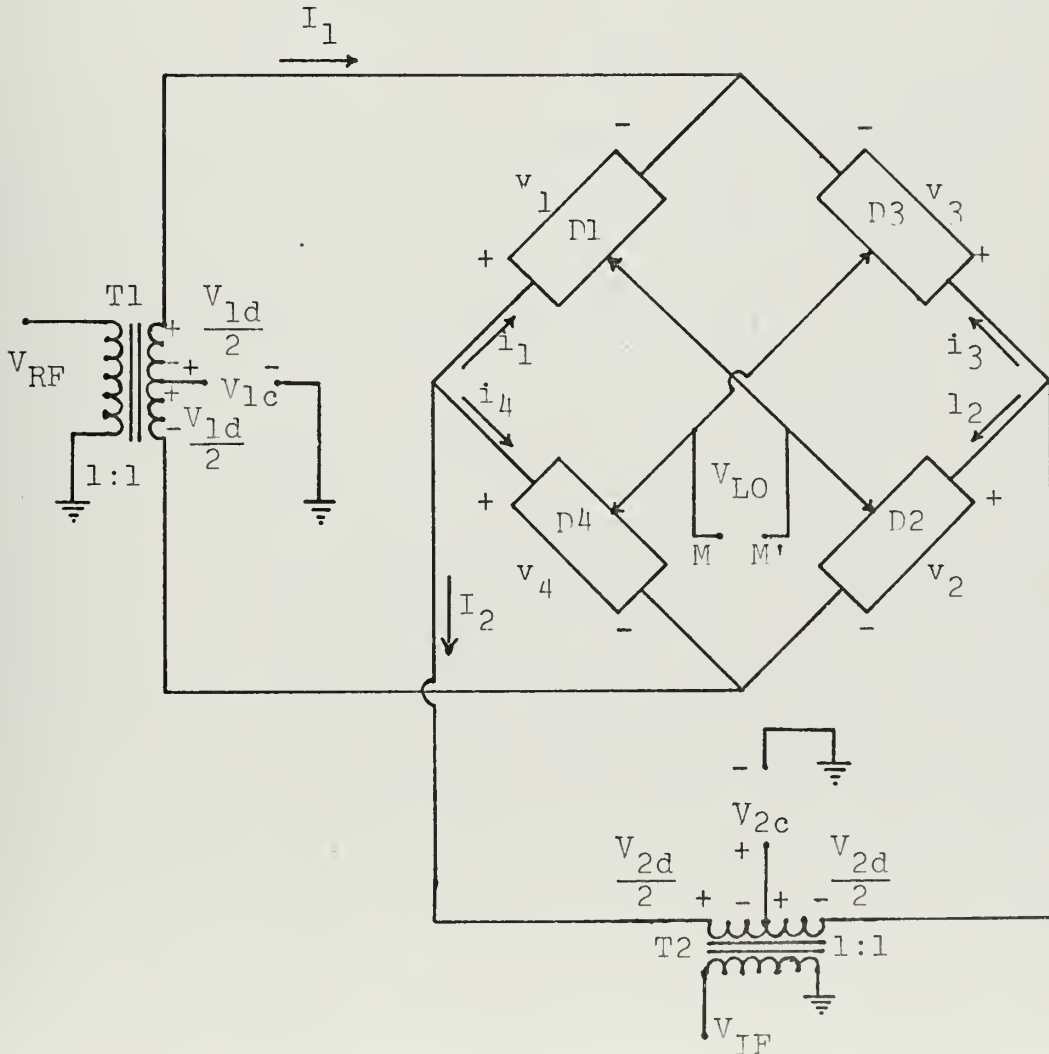


Figure 6. "ON-state" Current Flows and Voltage Drops.

both states of the mixer bridge; this allows separation of the effects of the terms which are converted by the mixer and those which are not. The voltage drops across the "ON" devices are written as a function of current; dividing them by their instantaneous currents define them as external impedances.

For state-1, with devices D_1 and D_2 "ON" and D_3 and D_4 "OFF," $I_1 = I_2$,

$$V_{1c} + \frac{V_{1d}}{2} + v_1 - \frac{V_{2d}}{2} - V_{2c} = 0 , \quad (\text{II-10})$$

$$V_{1c} - \frac{V_{1d}}{2} + v_2 + \frac{V_{2d}}{2} - V_{2c} = 0 . \quad (\text{II-11})$$

For state-2, with D_1 and D_2 "OFF" and D_3 and D_4 "ON,"

$$I_1 = -I_2 ,$$

$$V_{1c} + \frac{V_{1d}}{2} + v_3 + \frac{V_{2d}}{2} - V_{2c} = 0 , \quad (\text{II-12})$$

$$V_{1c} - \frac{V_{1d}}{2} + v_4 - \frac{V_{2d}}{2} - V_{2c} = 0 . \quad (\text{II-13})$$

v_1, v_2, v_3 and v_4 represent the small voltage drops across the devices in the "ON" state. It is assumed that they can be written as functions of their currents; and by comparing the polarity of the currents that pass through the individual devices when they are "ON,"

$$v_1 = f(-I_1) = f(-I_2) , \quad (\text{II-14.a})$$

$$v_2 = f(I_1) = f(I_2) , \quad (\text{II-14.b})$$

$$v_3 = f(-I_1) = f(I_2) , \quad (\text{II-14.c})$$

and

$$v_4 = f(I_1) = f(-I_2) . \quad (\text{II-14.d})$$

Then

$$v_1 = \frac{1}{2} [f(-I_1) + f(-I_2)] , \quad (\text{II-15.a})$$

$$v_2 = \frac{1}{2} [f(I_1) + f(I_2)] , \quad (\text{II-15.b})$$

$$v_3 = \frac{1}{2} [f(-I_1) + f(I_2)] , \quad (\text{II-15.c})$$

and

$$v_4 = \frac{1}{2} [f(I_1) + f(-I_2)] . \quad (\text{II-15.d})$$

Let

$$f(I) = f_e(I) + f_o(I) \quad (\text{II-16})$$

where $f_e(I) = f_e(-I)$ and $-f_o(I) = f_o(-I)$. The state-1 constraints become:

$$\begin{aligned} V_{1c} + \frac{V_{1d}}{2} + \frac{1}{2} [f_e(-I_1) + f_o(-I_1) + f_e(-I_2) + f_o(-I_2)] \\ - \frac{V_{2d}}{2} - V_{2c} = 0 \end{aligned} \quad (\text{II-17})$$

and

$$\begin{aligned} V_{1c} - \frac{V_{1d}}{2} + \frac{1}{2} [f_e(I_1) + f_o(I_1) + f_e(I_2) + f_o(I_2)] \\ + \frac{V_{2d}}{2} - V_{2c} = 0 . \end{aligned} \quad (\text{II-18})$$

Adding (II-17) and (II-18) gives

$$V_{1c} + \frac{1}{2} f_e(I_1) = V_{2c} - \frac{1}{2} f_e(I_2) , \quad (\text{II-19})$$

while subtracting gives

$$V_{1d} - f_o(I_1) = V_{2d} + f_o(I_2) . \quad (\text{II-20})$$

Following the same procedure for state-2 the constraints become:

$$\begin{aligned} V_{1c} + \frac{V_{1d}}{2} + \frac{1}{2} \left[f_e(-I_1) + f_o(-I_1) + f_e(I_2) + f_o(I_2) \right] \\ + \frac{V_{2d}}{2} - V_{2c} = 0 \end{aligned} \quad (\text{II-21})$$

and

$$\begin{aligned} V_{1c} - \frac{V_{1d}}{2} + \frac{1}{2} \left[f_e(I_1) + f_o(I_1) + f_e(-I_2) + f_o(-I_2) \right] \\ - \frac{V_{2d}}{2} - V_{2c} = 0 , \end{aligned} \quad (\text{II-22})$$

and after adding and subtracting (II-21) and (II-22),

$$V_{1c} + \frac{1}{2} f_e(I_1) = V_{2c} - \frac{1}{2} f_e(I_2) \quad (\text{II-23})$$

and

$$V_{1d} - \frac{1}{2} f_o(I_1) = -\left[V_{2d} + f_o(I_2) \right] . \quad (\text{II-24})$$

It becomes clear that the even-order voltage components are not affected by the state change while the odd-order components have reversed polarity. Therefore the odd-order voltages must be in series with the input voltage while the even-order voltages remain unconverted, and do not show up in the total input voltage. The effects of these "ON-state" voltages can be removed from the mixer and modeled by external voltage sources, or (if divided by their currents I_1 and I_2) impedances as shown in Figure 7.

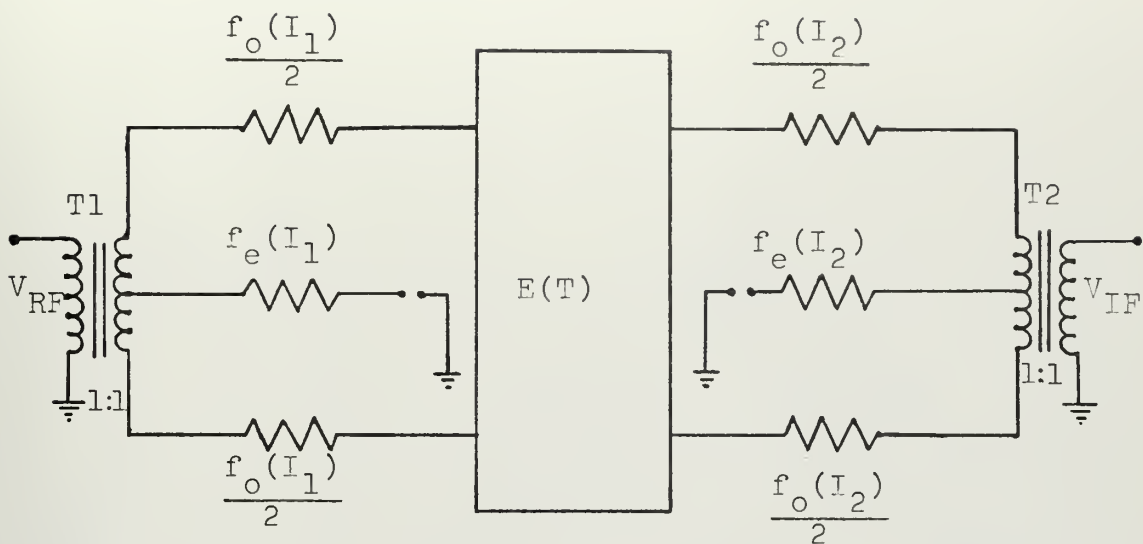


Figure 7. "ON-state" Voltage Drops Model.

A similar method is used for finding the effects of the "OFF-state" current flow based on the common-mode and difference-mode currents indicated in Figure 8. Some addition has already taken place at the input and output transformers with the result that the form of the equations will be slightly different with these given variables; however, the equations are consistent with the devices and circuits, and the results are similar: the even-order currents are not converted and appear in the center of the input and output transformers while the odd-order terms add to or subtract from the input currents and their effects are converted. In detail, the method involves summing the currents at each node. For state-1, nodes "P" and "Q" collapse to node "PQ" and nodes "R" and "S" to node "RS" indicated in Figure 9. For state-2, nodes "Q" and "R" become node "QR" and nodes "P" and "S" become node "PS" indicated in Figure 10.

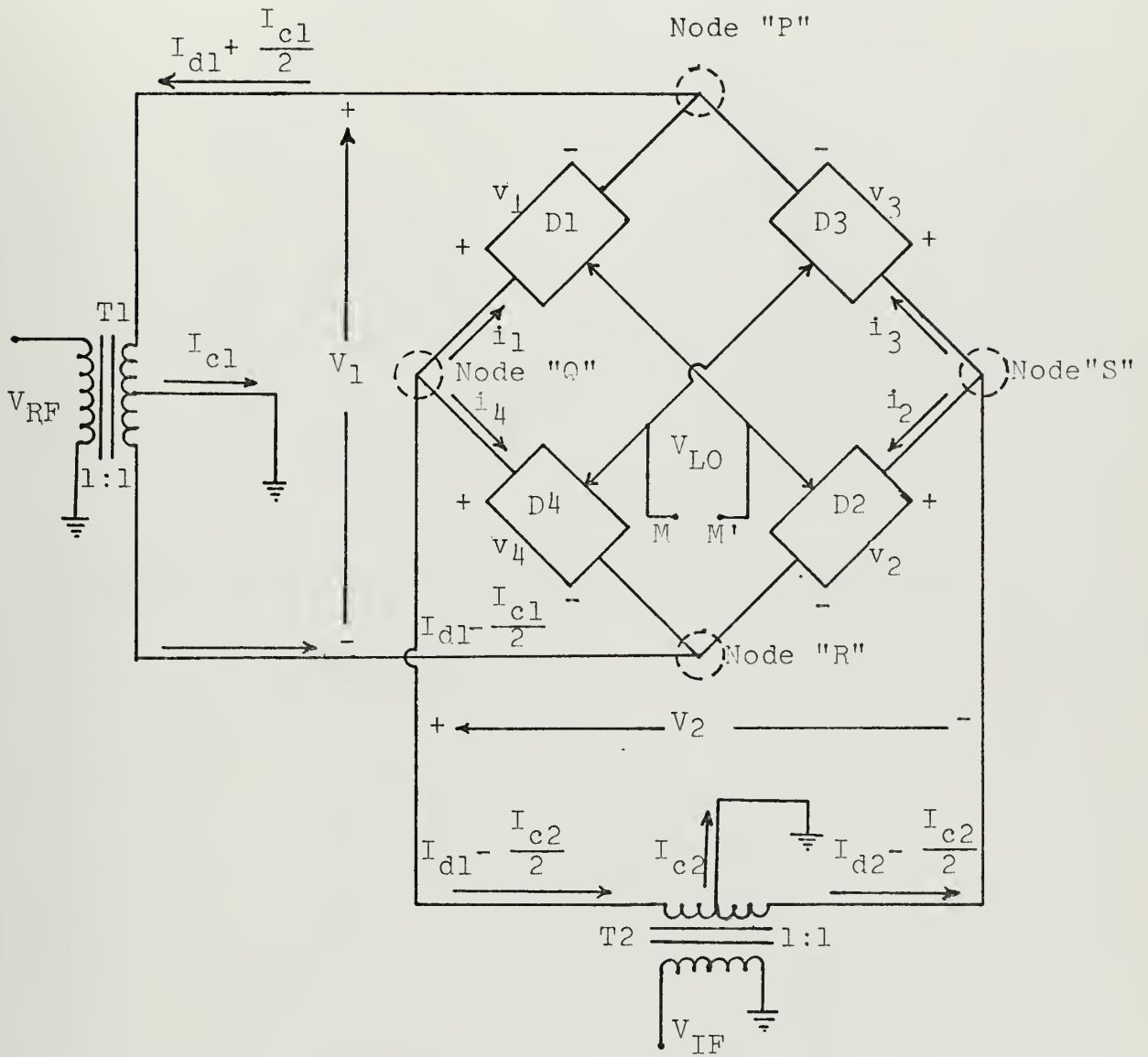


Figure 8. "OFF-state" Current Flows and Voltage Drops.

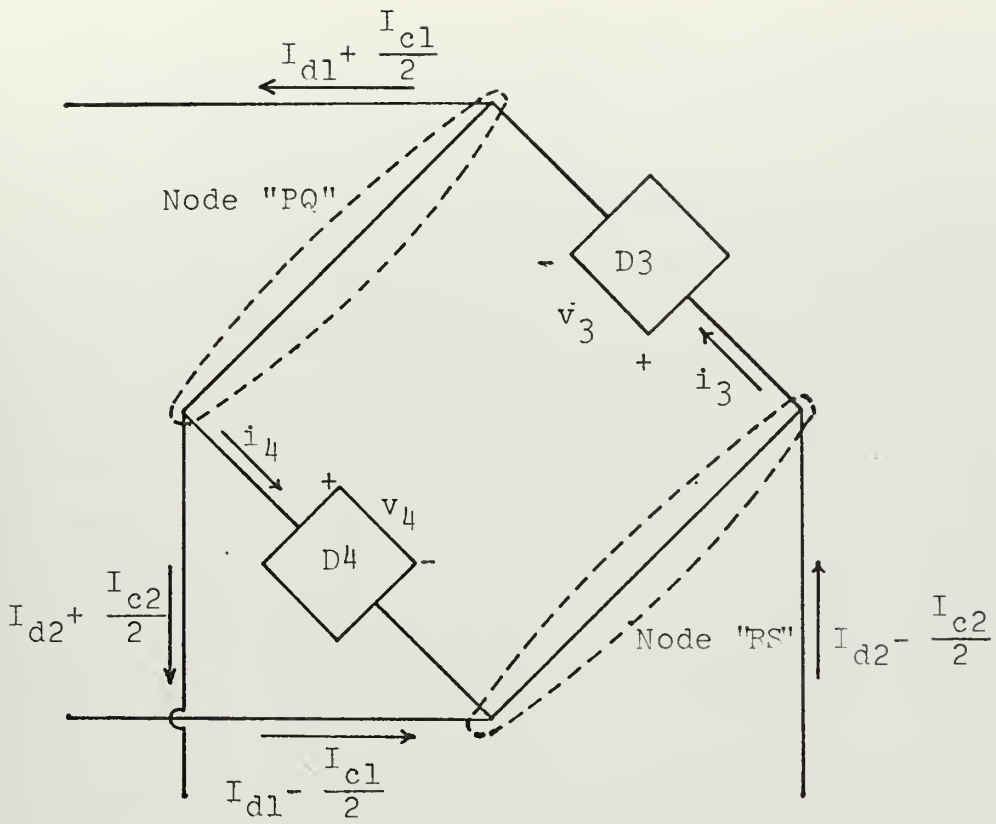


Figure 9. State-1 Current Flows and Voltage Drops.

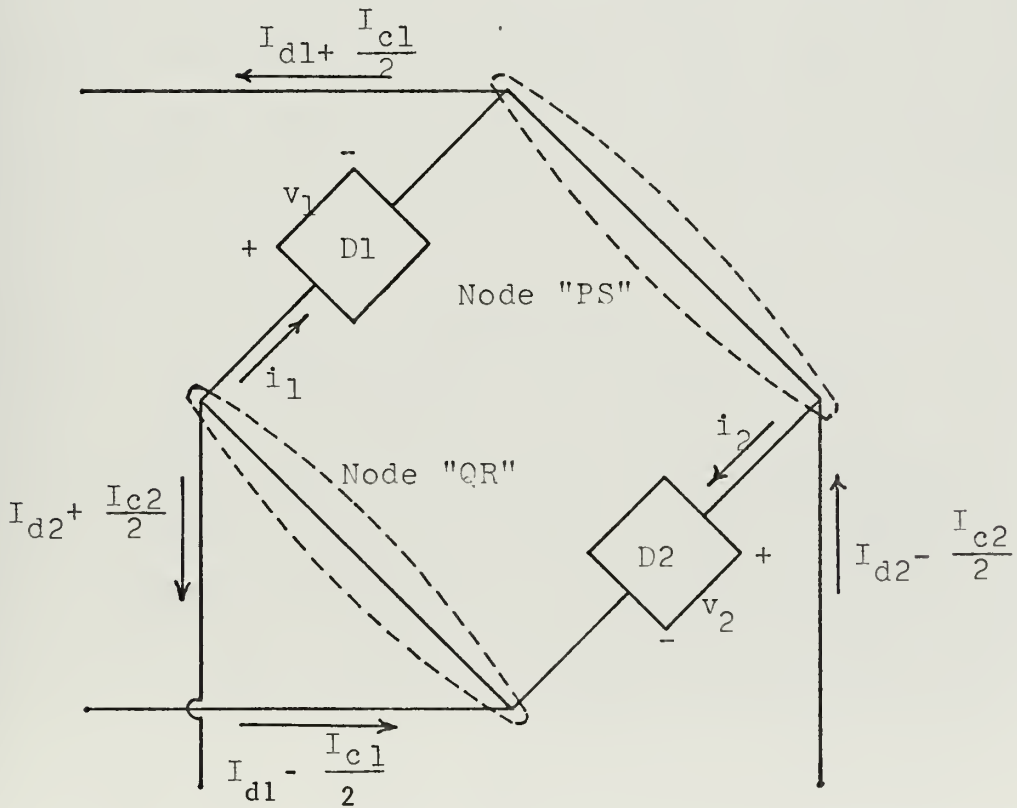


Figure 10. State-2 current Flows and Voltage Drops.

Then, the effects of the even-order term $h_e(V)$ and odd-order term $h_o(V)$ are shown in Figure 11.

The result is a first-order approximation to the effects of the parasitic impedances. For a more accurate iterative solution, the voltage across the h functions must be modified by the voltage drops of the "ON" devices. The external-source derivations were done independently and the total mixer characterization is shown in Figure 12. The h function across the input and output now becomes $h_o[V-f_o(I)]$ and the f becomes $f_o[I-h_o(V)]$. The substitutions are continued until the values converge.

The IM products generated in the parasitic impedances have one important difference from the IM as analyzed in the simple nonlinear resistance in the Appendix A. Since the frequency conversion follows the odd-order impedance at the input, one pass through the $E(T)$ conversion is sufficient for IM generation at the output. Similarly, the third-order

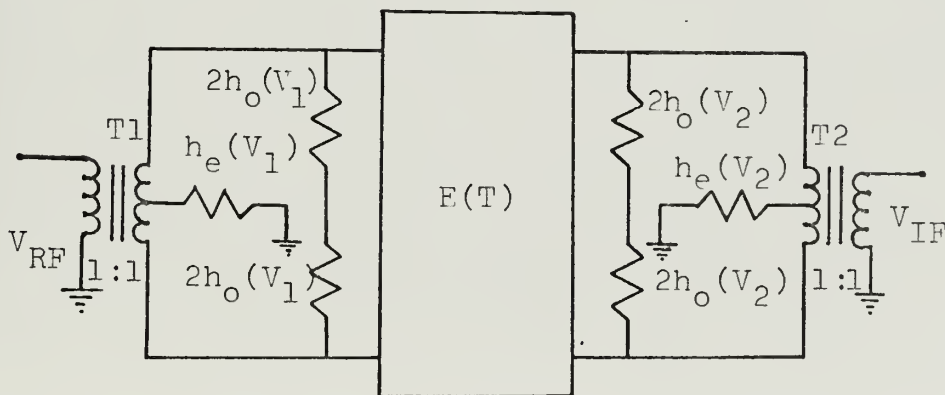


Figure 11. "OFF-state" Current Flows Model.

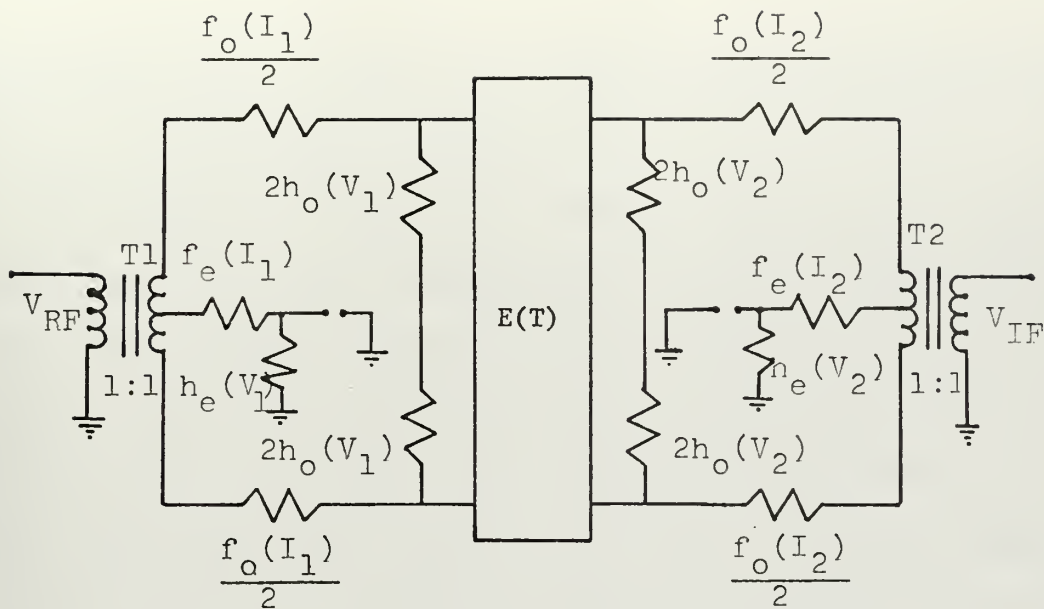


Figure 12. The Total Mixer Characterization.

term in the parasitic impedance at the output takes the undesired signals, converted to frequencies $f_{LO} \pm f_m$ and $f_{LO} \pm f_n$ and converts them to frequencies of the form: $2[f_{LO} \pm f_m] \pm [f_{LO} \pm f_n]$ which includes a component at $f_{LO} - [2f_m \pm f_n] = f_{IF}$. Both odd-order impedances on input and output contribute to the generation of third-order IM.

The conversion loss of the mixer because of parasitic impedances will be greater than zero. In practice the major contribution to conversion loss is the "ON-state" resistance, in the FET, fixed by the minimum channel resistance. The "OFF-state" series resistance is on the order of several thousand ohms or more and the capacitive reactance to ground is of the same magnitude in a typical FET. A good estimate of the conversion loss, therefore, simply models the mixer as the input voltage source (with its internal generator

resistance R_g) in series with the "ON-state" resistance R_{ON} (or Z_{ON} for general solution).

The conversion loss is a difficult quantity to measure, depending on an exact knowledge of the mixer output impedance; more readily available is the transducer loss, the ratio of available input power to actual output power into the load resistance R_L . The available input power is $|V_{in}|^2/4R_g$ while the actual output power is $|V_{out}|^2/2R_L$. If one assumes the frequency terminations used in the experimental work, of short circuited sum at the output and open circuited image at the input, the output impedance $Z_{out} = \frac{\pi^2}{4} [R_g + Z_{ON}]$ (Figures 13 and 14).

The input voltage V_{in} transforms to a voltage generator of $\frac{2}{\pi} V_{in}$ in series with Z_{out} , and the output voltage:

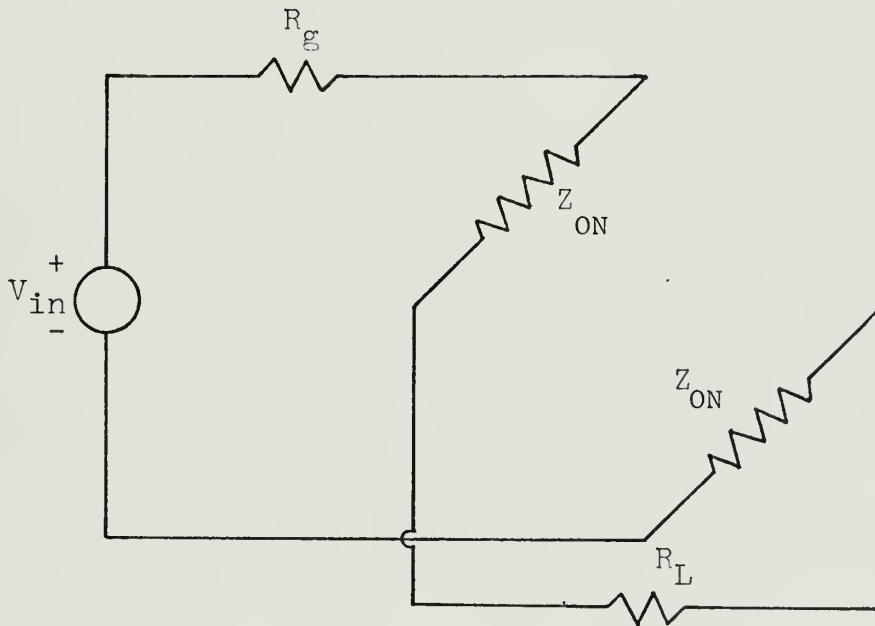


Figure 13. State-1 Equivalent Circuit with $Z_{ON} > 0$ and $Z_{OFF} = \infty$.

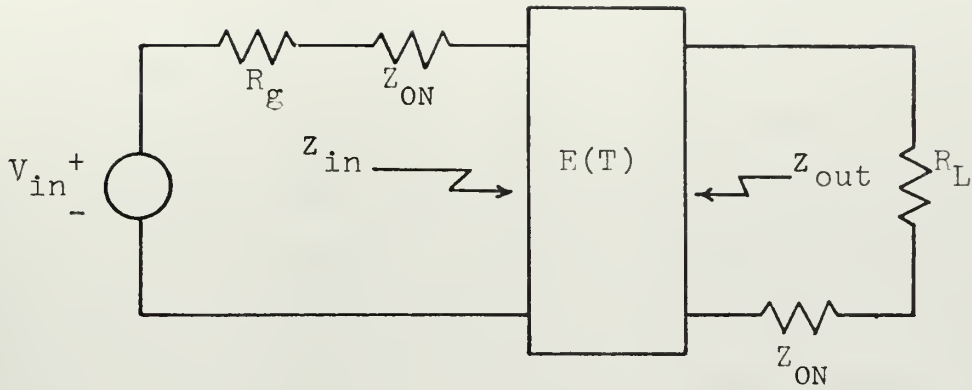


Figure 14. Output Impedance Calculation.

$$V_{out} = \frac{\frac{2}{\pi} V_{in} R_L}{R_L + Z_{ON} + \frac{4}{\pi^2} [Z_{ON} + R_g]}, \quad (II-25)$$

then transducer loss is

$$L_T = \frac{P_{IN}}{P_{OUT}} = \frac{\pi^2 [R_L + Z_{ON} + \frac{4}{\pi^2} (R_g + Z_{ON})]^2}{8 R_g R_L}$$

C. INTERMODULATION DISTORTION

IM distortion is analyzed in two ways. The first one is according to the nonlinear properties of MOSFETs and the second one according to the "OFF-state" parasitic capacitance of MOSFETs.

The simplest mechanism for generation of IM distortion is the third-order term in a V-I relationship describing the operation of the MOSFET. As has been shown for nonlinear resistance in Appendix A, the third-order V^3 or I^3 terms produce voltages or currents at f_m , f_n , $3f_m$, $3f_n$, $2f_m + f_n$ and

$2f_n \pm f_m$. With IM defined in the normal way, with $2f_m \pm f_n = f_{RF}$, the IM products must still be converted to the IF frequency by a second-pass through the square-law portion of the converter. The mixer must then be modeled either as a series connection of an odd-order nonlinear impedance with the corresponding even-order impedance or a series connection of two nonlinear impedances; the first of which produces the IM and the second which converts the IM down to the IF frequency.

Most analyses of mixer IM generation assume that an input consisting of the LO signal and two IM-producing undesired signals will give an output at the IF frequency. However, a detailed expansion of $V_{in} = V_{LO} \cos \omega_{LO} t + V_3 \cos \omega_3 t + V_4 \cos \omega_4 t$ shows that instead, the mixer produces a large number of terms corresponding to the input frequencies times one, two or three and one, two or three at a time such that the total of the ω coefficients absolute values is either one or three.

If one now allows some feedback mechanism to return these signals to the input, a large number of frequency combinations will produce IM power at the IF, the total power being the sum of the individual contributions, with proper regard for the frequency dependencies of the feedback network and the relative phases and possible cancellations of separate terms.

Let

$$V_{out} = r_0 I + r_1 I^2 + r_2 I^3 \text{ -----} \quad (II-27)$$

The linear and square terms will produce the same frequency terms examined in the Appendix A. If it is assumed that

there is no second harmonic feedback, the IM will be generated by the cubic term $r_2 I^3$. Then, let $V_{\text{out(cubic)}} = r_2 I^3$ and

$$V_{\text{out(cubic)}} = r_2 \left[I_{L0} \cos \omega_{L0} t + I_1 \cos \omega_1 t + I_2 \cos \omega_2 t \right]^3 \quad (\text{II-28})$$

where I_1 and I_2 are some undesired signals at the third-order IM frequencies $2f_1 - f_2 = f_{\text{RF}}$.

The expansion of the cubic term follows:

$$\begin{aligned} (a+b+c)^3 &= a^3 + b^3 + c^3 + 3a^2c + 3ac^2 + 3b^2c + 3bc^2 + 3a^2b \\ &\quad + 3ab^2 + 6abc \quad . \end{aligned} \quad (\text{II-29})$$

Letting $a = I_{L0} \cos \omega_{L0} t$, $b = I_1 \cos \omega_1 t$ and $c = I_2 \cos \omega_2 t$ and recalling from trigonometry:

$$\cos^3 x = \frac{1}{4} (\cos 3x + 3 \cos x) \quad (\text{II-30.a})$$

and

$$\begin{aligned} \cos x \cdot \cos y \cdot \cos z &= \frac{1}{4} \left[\cos(x+y+z) + \cos(x-y-z) + \cos(x+y-z) \right. \\ &\quad \left. + \cos(x-y+z) \right]; \end{aligned} \quad (\text{II-30.b})$$

there are ten terms in the expansion of V_{out} . The first term is $(r_2 I_{L0}^3 / 4) (\cos 3\omega_{L0} t + 3 \cos \omega_{L0} t)$. The second and third terms are of the same form; with the interchange I_1 and ω_1 and I_2 and ω_2 for I_{L0} and ω_{L0} . The fourth term is of the form $(3/2) I_1^2 I_2 \cos \omega_2 t + (3/4) I_1^2 I_2 [\cos(\omega_2 + 2\omega_1) t + \cos(\omega_2 - 2\omega_1) t]$. The fifth through ninth terms are similar in form with the correct currents and frequencies inserted. The tenth term is,

$$\begin{aligned} (6/4) I_{L0} I_1 I_2 &\left[\cos(\omega_{L0} + \omega_1 + \omega_2) t + \cos(\omega_{L0} - \omega_1 - \omega_2) t \right. \\ &\quad \left. + \cos(\omega_{L0} + \omega_1 - \omega_2) t + \cos(\omega_{L0} - \omega_1 + \omega_2) t \right]. \end{aligned}$$



Since $f_{IF} = f_{LO} - f_{RF}$, for third-order IM output at the IF frequency one must convert down to the frequency $f_{IF} = f_{LO} - (2f_1 - f_2)$. This frequency can be obtained adding and subtracting other frequencies from the frequency of the expansion terms in a square-law device generating terms of the form $\cos(x \pm y)$. That is, before getting any output at the IF frequency, one must add or subtract other first-order or third-order terms from the terms of the cubic expansion, the addition or subtraction taking place in a square-law characteristic. The total IM voltage at the output port is then the sum of the individual powers.

Third-order IM is thus seen to be a highly complicated phenomenon, with a number of variables that are not always easily described. The IF frequency term can be assembled many ways, with varying amplitudes for each combination; but all combinations require a second-pass through the square-law portion of the mixer. If the IM products can be assumed to pass through the mixer twice (and they must to produce an output at the IF frequency) one suspects it is possible for them to pass through the mixer three times. This double feedback loop introduces the possibility of IM in a perfect square-law device. Suppose the second harmonic current generated by the square-law mixer characteristic is fed back to the input through some feed-back coefficient k . The input port now has available signals at one frequency and twice some other frequency, if these are the standard undesired IM frequencies chosen so that $2f_m - f_n = f_{RF}$, then the

output port will have available power at the difference frequency, generated by the square-law characteristic of the mixer. The final assumption holds that this difference frequency is also allowed to feed back into the input where it combines with the LO frequency to produce a signal at $f_{LO} - (2f_m - f_n) = f_{IF}$. If care is taken with the second harmonic terminations in the mixer, the feed-back coefficients will be extremely small, and the IM generated by the second harmonic behavior will be much less than that generated by the normal third-order mechanism or eliminated.

At this point, the IM generated in odd-order "OFF-state" reverse transconductances is analyzed. It is found from theoretical consideration that the "OFF-state" parasitic capacitance provides the fundamental limit in a MOSFET mixer as in a diode mixer, generating IM at levels, typically 60 dB below the signal level. It is possible to derive the polynomial coefficients for the MOSFET drain-to-source capacitance as the Taylor series coefficients of an expansion of the incremental capacitance as a function of the MOSFET drain-to-source voltage around some fixed value such as $V_{DS} = 0$.

The physical mechanisms of the MOSFET allow only second-order effects for cubic and higher terms in a power series expansion of the drain-to-source capacitance C_{DS} . To estimate the effects of the higher order terms in the C_{DS} polynomial with the MOSFET in the "OFF-state," the incremental capacitance is measured as a function of V_{DS} on a capacitance

bridge. This measures incremental capacitance, C_{inc} , as the partial derivative of charge with respect to the voltage at some C_0 and bias voltage V_0 . The points of Q/V are operated upon by the method of divided differences to obtain a polynomial expression for the incremental capacitance as a function of V_{DC} . If

$$\frac{Q}{V} = a+bV+cV^2+dV^3+ \text{-----} \quad (\text{II-31})$$

then total capacitance (the desired capacitance) can be written as a polynomial expansion around $V = 0$,

$$C(V) = C_0+C_1V+C_2V^2+C_3V^3 \text{-----} . \quad (\text{II-32})$$

Then all the C_i are constants and one can write $Q(V) = VC(V)$ and

$$\frac{Q(V)}{V} = C(V) = C_0+2C_1V+3C_2V^2+ \text{-----} . \quad (\text{II-33})$$

Hence $C_0 = a$, $C_1 = b/2$, $C_2 = c/3$, etc., and complete expression for the total capacitance as a function of the DC bias voltage over some range near $V = 0$ results. The current through the channel is then $\frac{d[Q(V)]}{dt}$ and the IM current is equal to $\frac{d}{dt} [C_2V^3]$ where V is the total instantaneous voltage across the drain-to-source. If $V = V_m \cos \omega_m t + V_n \cos \omega_n t$ for third-order IM with $2f_m - f_n = f_{RF}$, then the IM current is

$$\begin{aligned} I_{IM} &= \frac{d}{dt} [C_2 \frac{3}{4} V_m^2 V_n \cos(2\omega_m - \omega_n)t] \\ &= - \frac{3}{4} C_2 V_m^2 V_n (2\omega_m - \omega_n) \sin(2\omega_m - \omega_n)t , \end{aligned} \quad (\text{II-34})$$

where $2\omega_m - \omega_n = \omega_{RF}$. Letting the m and n frequencies have equal amplitudes, $V_m = V_n = V$ and the IM current amplitude is,

$$I_{IM} = \frac{3}{4} C_2 V^3 \omega_{RF} . \quad (II-35)$$

Since the parasitic impedance is across the input port, the voltage across it is approximately the same as the voltage across the load resistance and $V = (V_{in} R_{in}) / (R_{in} + R_g)$ as shown in Figure 15.

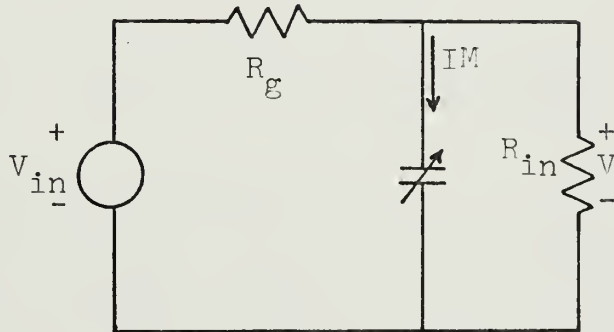


Figure 15. Circuit for Varactor IM Calculation.

The signal current in the load resistance (here designated R_{in} , the input resistance of the mixer from the load resistance transformed bi-laterally) is approximately

$$I_{in} = V_{in} / (R_{in} + R_g). \quad \text{Then dynamic range, D.R., is equal to}$$

$$\left| I_{in} \right|^2 / \left| I_{IM} \right|^2,$$

$$\begin{aligned}
 \text{D.R.} &= \frac{|I_{in}|^2}{|I_{IM}|^2} = \frac{|V_{in}/(R_{in}+R_g)|^2}{\left| \frac{3}{4} C_2 \omega_{RF} \left[\frac{V_{in} R_{in}}{(R_{in}+R_g)} \right]^3 \right|^2} \\
 &= \frac{16}{9} \frac{(R_g+R_{in})^4}{C_2^2 V_{in}^4 R_{in}^2 \omega_{RF}^2} .
 \end{aligned} \tag{II-36}$$

For matched conditions, $R_{in} = R_g$,

$$\text{D.R.} = \frac{256}{9} \frac{1}{C_2^2 V_{in}^4 R_g^2 \omega_{RF}^2} . \tag{II-37}$$

It appears, then, the fundamental limit on the D.R. of an FET operating as a mixer with the signal at the source is the incremental drain-to-source capacitance, C_{DS} .

D. SECOND HARMONIC TERMINATION

The second harmonic behavior of the mixer because of the even-order terms in the center-taps of the input and output transformers (see Figure 12) is not well understood. It is expected that grounding the center-taps of these transformers will provide maximum conversion gain and dynamic range by diverting the second harmonic currents to ground and the voltages to nearly zero at these terminals. This was proven to be true during experimental evaluation.

E. DEVICE LIMITATIONS

The greater part of the effort here is expended on calculating departures from ideal models, with perfect square-wave switching assumed.

It is unfortunately the case that no switching device is perfect. In general the "ON-state" will have a measurable voltage drop, and the "OFF-state" a measurable current, due to parasitic impedances in series and parallel with the ideal switch model of each device. A second departure from perfection has to do with the switching waveform. It is apparant from the foregoing discussion that the optimum waveform is a simple square-wave. The reversing switch model requires that equal time periods be spent in the "OFF" and "ON" states for each device, and it is evident that any transition time between states represents a time in which the device appears as some unspecified nonlinear resistance. This is undesirable, since this behavior causes conversion loss and subjects the mixer to IM generation while in the transitional state. In practice it is difficult to say much about the transition time behavior. There is another limitation on the power levels which the mixer can handle before the IM generated becomes measurable. The mixer has been characterized as if the only variables controlling the operating point were the switching waveform amplitudes. However, with high signal levels (both desired and undesired signals) the operating point will vary with the instantaneous amplitudes of the input signals. The problems arise when the switched states do not have an infinite range of voltage or current available over which the state remains unchanged and the signal level on the devices can drive them into nonlinear region indicated in Figure 16.

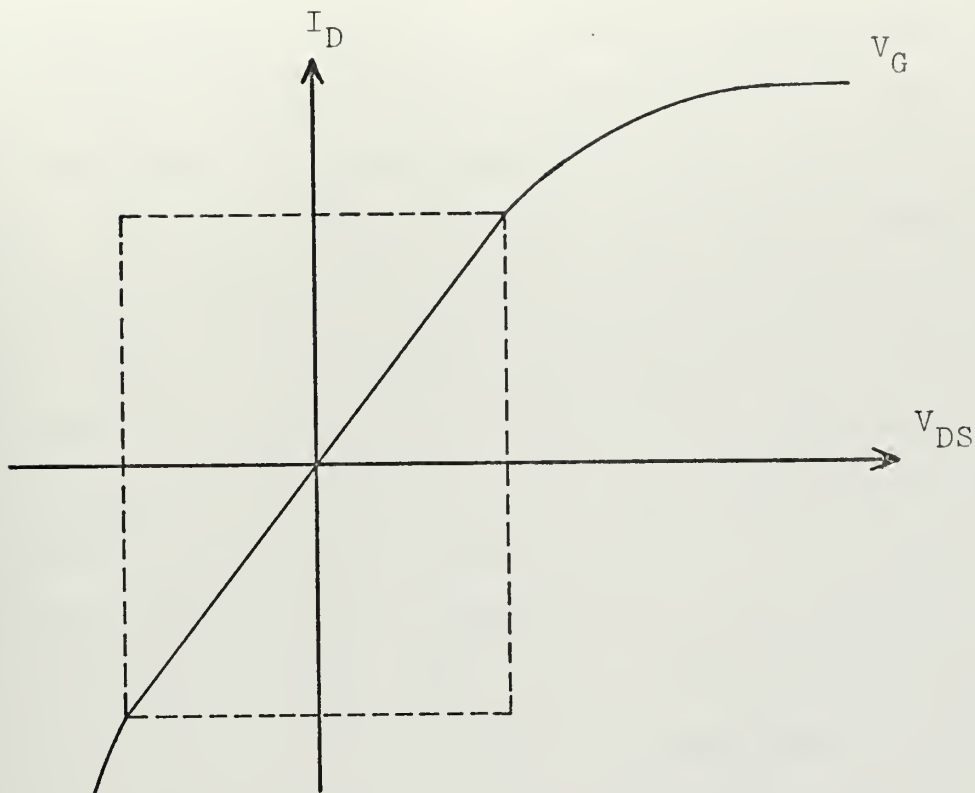


Figure 16. Usable Region of I_D - V_{DS} Curve (dotted area).

This mode of IM generation most closely approximates the normal modes of IM generation in conventional mixers, and it is not surprising that the best results and lowest IM occur with devices designed for minimum IM in conventional mixers. This large linear range in normal circuitry is another of the reasons for the choice of MOSFETs for the switched devices. The normal "ON-state" of an FET has a resistance greater than zero, on the resistive portion of the I_D versus V_{DS} curve. For large signals on the source (as in the bridge mixer) the operating point moves along the characteristic (fixed V_{gate}) into the nonlinear region, generating IM.

The final limitation on conversion gain and D.R. comes from the transition times associated with any real-world

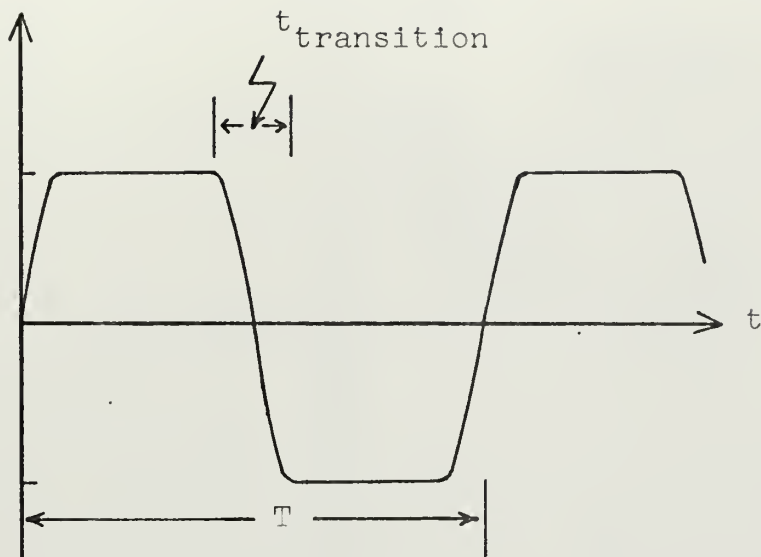
switching system. While the optimum LO waveform is a perfect square-wave, the combination of high required LO power and relatively high frequency make such a wave difficult to obtain. Much more likely to occur is a clipped sine-wave (as shown in Figure 17.a) with fairly long transition times, on the order of $T/6$ each way, and IM because of transition-time behavior is indicated in Figure 17.b. This means that the FETs spend a good fraction of time traveling through a succession of operating points somewhere in the normal operating region of their characteristic curve over a general area (as shown in Figure 18) fixed by the amplitude of the input signals at the source and the approximate path of the operating point between the "ON" and "OFF" states. The amplitude of the IM will be greatest when the FET is somewhere near the middle of the transition and the output amplitude may be approximated by triangles of base-width $t_{\text{transition}}$ and period $T/2$.

F. SUMMARY OF THEORETICAL ANALYSIS

The D.R. of the balanced-bridge MOSFET mixer is thus seen to be the range over which the mixer can operate without running into the device limitations. Conversion loss and system noise-figure set the lower limit on the sensitivity and IM generated by parasitic impedances, signal level-produced nonlinearities and transition time effects sets the upper limit of the D.R.

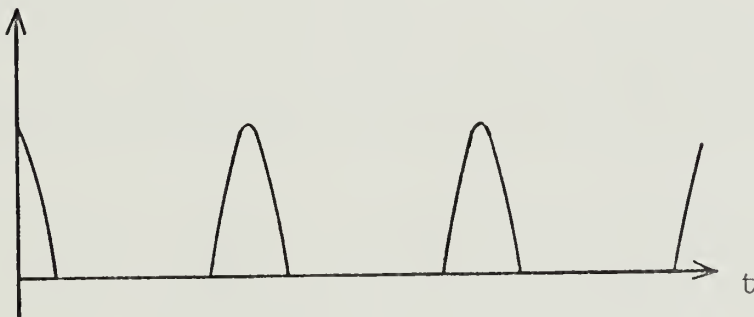
This portion of the thesis has developed the mathematical theory behind an unusual mixer circuit and shown that

LO Voltage
Amplitude



(a). LO Waveform.

IM Amplitude



(b). IM Because of Transition Time Behavior.

Figure 17.

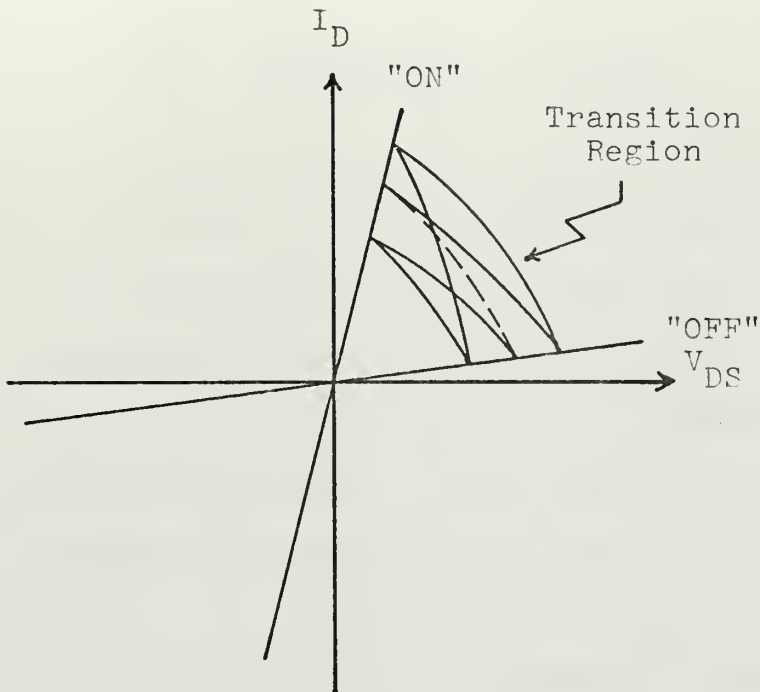


Figure 18. Transition Region.

the ideal model is free from IM and implies zero conversion loss. The departures from the ideal case have been analyzed in more or less detail and methods have been developed for estimating the conversion loss and D.R. of the resulting mixer.

The following section of this thesis is devoted to a description and explanation of the experiments conducted to measure the performance of a real-world version of this mixer.

III. EXPERIMENTAL PROCEDURE

Experimental systems should be capable of accurate measurement of as many of the experimental variables as possible. The main consideration of this thesis in the choice of components was to obtain minimum conversion loss with high port-to-port isolation with the widest possible dynamic range and band width. Experimental work was performed to verify the theoretical analysis and to make a comparison between a hot-carrier diode double-balanced mixer and the balanced-bridge switching-state MOSFET mixer.

A. MOSFETS

The MOSFETs used in this mixer were MOTOROLA 3N171 silicon N-channel, enhancement mode, insulated single gate, switching MOSFETs in a TO-72 metal package.

B. TRANSFORMERS

The transformers are wound on micro-metals, type T 37-13 (50-120 MHz), T 37-0 (100-200 MHz), T 50-10 (10-35 MHz) and T 44-10 (10-50 MHz) powdered iron toroidal cores.

Coupling between the wires directly affects the band width of the mixer. Thus, the windings must be as tight as possible for obtaining the desired wide band performance. This is accomplished by twisting the three wires together and tightly winding them on the toroid shown in the Figure 19. Twelve trifilar turns of number 27 enameled wire are wound

on each toroid. A schematic diagram of complete transformer identifies the primary, secondary and center-tap (CT) leads in Figure 20.

A one-to-one transformer ratio is selected because of ease in construction. Ratios other than one-to-one will affect the operating point of the MOSFET due to reflected and parasitic impedances and will change the drain current. Therefore, a transformation ratio other than one-to-one will result in only complicating the design in terms of balance. Toroid material choice is important in terms of conversion loss. The correct type of core material must be used in order to realize the highest possible tuned-circuit Q at a particular frequency range. Minimum interaction between the tuned stages is usually of paramount importance to the designer. There is no simple rule that can be used for selecting a toroid core for a particular job. Many things must be considered, notably the intended frequency of operation, the operating frequency versus the physical size and permeability of the core. The higher the permeability of the material, the fewer the number of turns required. In the VHF range, minimum I^2R loss is desirable, therefore, smaller cores with high permeability should be used. High- Q toroidal transformers can assure good image rejection, efficiency and extremely stable inductances over a wide temperature range. The cores used in this experiment have an average Q of 175.

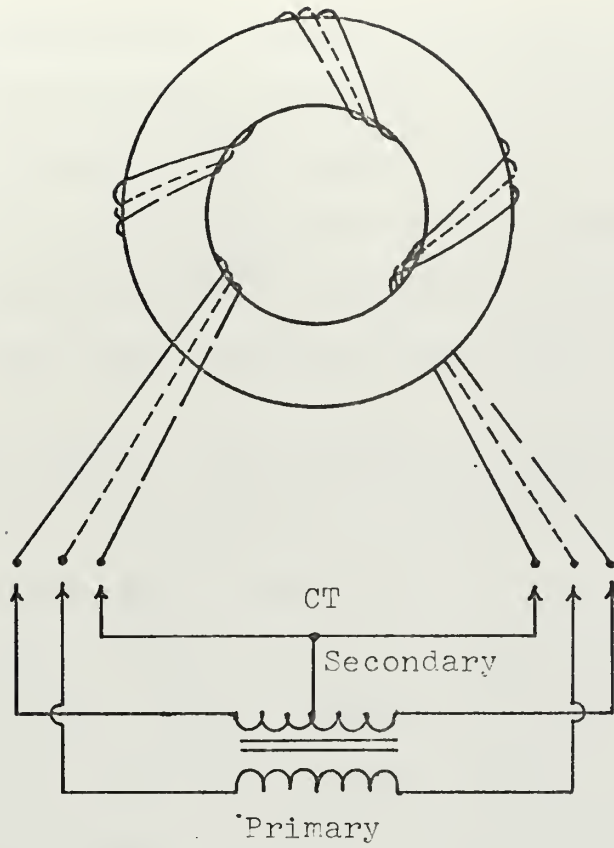


Figure 19. Toroid Winding (wires are shown untwisted for clarity).

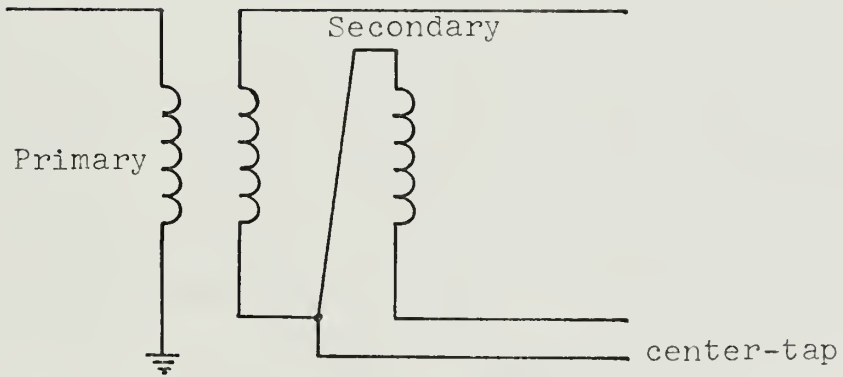


Figure 20. Schematic Showing the Connections of the Trifilar Windings.

In this investigation, various materials and sizes were tested to determine effect of toroids on conversion loss. A 15 dB range in loss values demonstrated the major influence of transformer core configuration. These experiments also showed that wide band width is obtained by designing toroidal transformers with tight coupling between the windings.

C. EXPERIMENTAL SET-UP, EXPERIMENT AND LIMITATIONS

An experiment was conducted in the 10 to 200 MHz range using the set-up shown in Figure 21.

The signal generators used are HP model 608 C VHF signal generators with power output limited at 7 dbm. The IF output was fed into 50 ohm Tektronix type 491 spectrum analyzer. The LO power was taken from a Boonton 2 watt power amplifier fed by a signal generator. One unfortunate limitation of this arrangement is the high noise level in the output of the power amplifier. Ordinarily this would be no problem since mixer sensitivity is uneffected. However, if there is a strong signal near the frequency of the desired signal, the LO noise will be converted to the output frequency. If the frequency difference between the two signals is "W" KHz, the converted noise will be the power level of the undesired signal times the power level of the noise "W" KHz away from the LO center frequency. If the desired signal is only a few dB above the noise level, it will be masked by this noise. The most direct solution is to use a narrow-band LO power source, one designed for

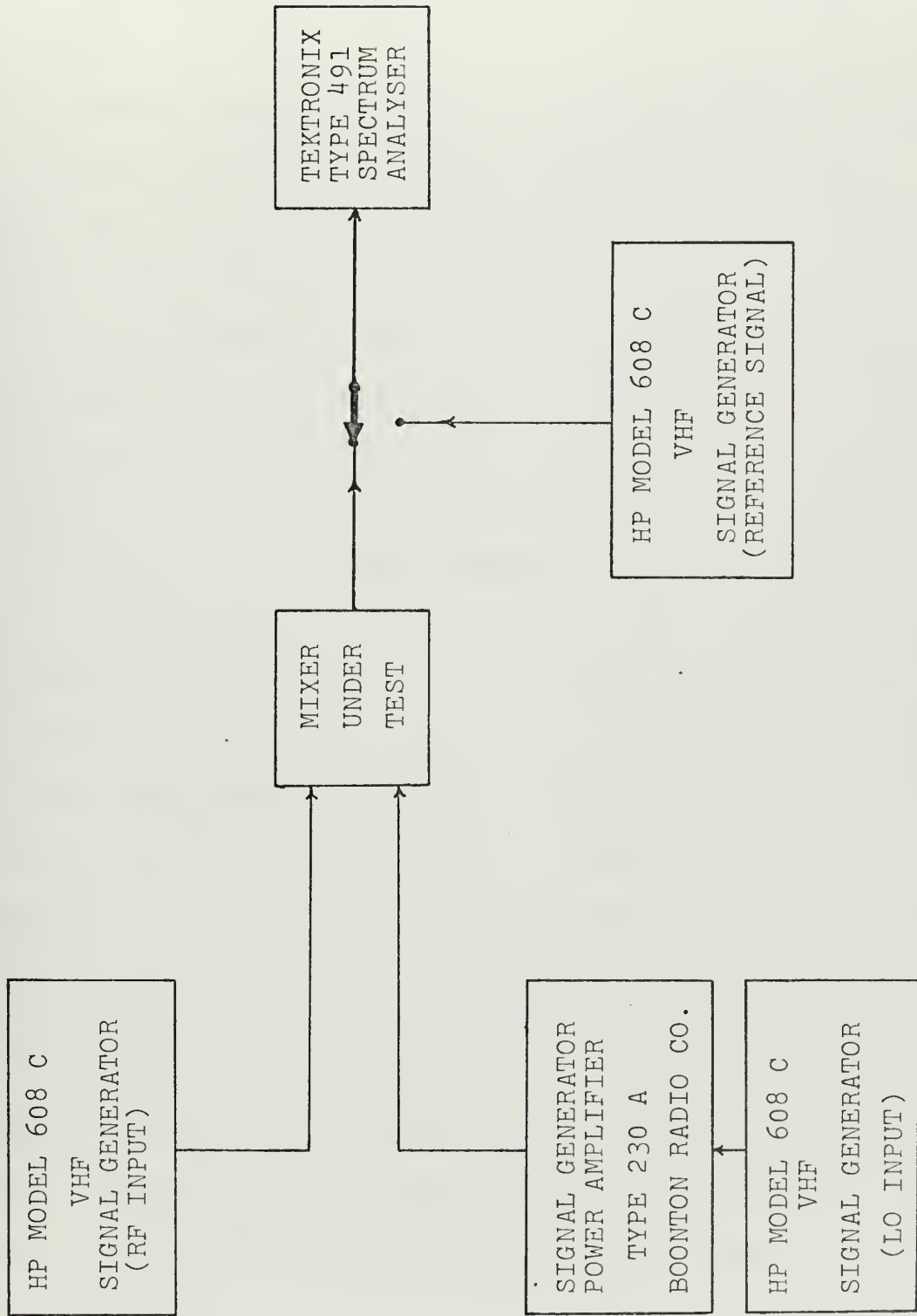


Figure 21. Experimental Set-up.

minimum noise output. This problem is not basic to the mixer, but involves the development of low-noise power amplifiers.

The mixer (under test) used in this experiment was based on a bridge of four MOSFETs, fed directly by the signal generators. The RF input was applied to the sources and the IF output taken from the drains. The substrates were biased at -1 volt DC from a 15 volt DC power supply for minimum conversion loss. The paired leads of substrates are isolated by 100 Kohm resistances shown in Figure 3; this isolation is important, based on the MOSFET physical model. The LO was fed to the gates of the four MOSFETs in alternate pairs. The gates themselves are DC-coupled so that they may be DC biased individually by the symmetric bias network shown in Figure 4. Gate bias was +4 volt DC. Although the gates DC bias voltages were made independently adjustable by three identical variable potentiometers with the goal of matching gate turn-on characteristics, the actual voltage levels are same (4 volts DC), for making conversion loss minimum. One suspect that bias potential adjustment is a matter of matching and cancelling coefficients of the nonlinear resistance power series expansion of the MOSFETs drain current (I_D) versus drain-to-source voltage (V_{DS}) curve (see Figure 16). It is not clear whether this is effective on the third-order terms in direct IM production and cancellation or on the cancellation of the second harmonic terms at the symmetric points of the balanced-bridge. In any case, adjustment of the bias

potentiometers for minimum measured conversion loss and IM allows a large extension of dynamic range of the mixer. For high signal levels, the operating points of the MOSFETs are perturbed by the signal levels, and coefficients change, moving the IM out of the gate bias null. The result is that the IM may be nulled down to an unmeasurable level at some arbitrary signal level, and it will increase if the drive level is raised. Conversion loss in this case was increased as mentioned before in Section II-E.

The LO input (port) network is set as shown in Figure 22. Two 100 ohm-2 watt resistances are included in this configuration because a power amplifier was employed for driving gates at the LO switching rate. This was accounted for when recording the experimental voltage data at points M and M'. The IF output is short-circuited at the sum frequency by a parallel-tuned LC circuit set for the 30 MHz frequency. The RF input, LO input and IF output ports have 50 ohm toroidal transformers. The reference generator was set to

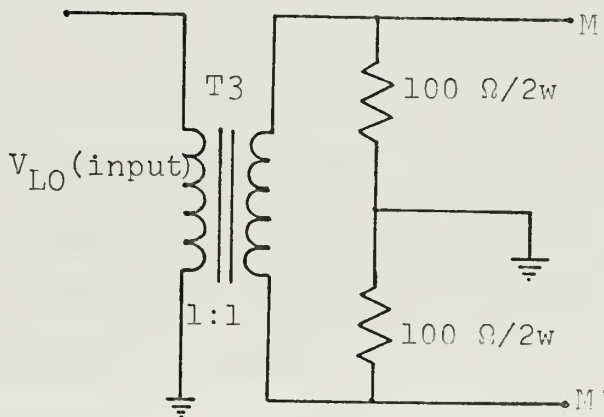


Figure 22. LO Input Network.

the 30 MHz IF frequency and used for measuring the output power of the mixer by the comparison method. Since the difference in RF input and IF output gives the conversion loss, this information was also obtained. Isolation was measured in the same manner.

Additional limiting effects for the 190 MHz bandwidth are the toroids used and the layout. The circuit-board design depends upon which ports of the mixer circuit are used as RF, LO, and IF. Since the mixer is bi-lateral, a symmetrical design is difficult to achieve, although very important, as was discovered in the printed-circuit layout. The initial PC configuration conversion loss was improved 6 dB by a second layout in which careful attention was given to symmetry.

Table I indicates there is a 3 dB difference in conversion loss between the theoretical and measured values for the MOSFET mixer. This difference varies irregularly in RF and LO isolation for all mixer types. This difference is caused by stray capacitances (circuit-board design effect), by transformer losses (toroid effect), by impedance mismatching, parasitic impedance behavior, reflected impedance and by possible measurement error. At frequencies out of the 10-200 MHz range losses increase rapidly.

The dynamic range of a mixer is a function of LO power and IM and spurious responses. Due to the limited output of the signal generators, the upper limit of the dynamic range was restricted to 0 dbm. The lower limit was -50 dbm, set by the noise figure of the spectrum analyzer.

D. RESULTS AND COMPARISON

Measured 30 MHz IF output power versus RF input power plots are shown in Figure 23 and 24 for the MOSFET mixer at different frequencies between 10-200 MHz, with 18 and 25 dbm LO power, respectively. It is observed that IF power versus RF power plots for the $f_{RF} = 10-50$ MHz and $f_{LO} = 40-70$ MHz ranges are exactly the same as in Figure 23 with 18 dbm LO power. It is also observed that the $f_{RF} = 75-150$ MHz and $f_{LO} = 105-180$ MHz ranges are almost the same as in Figure 24 with 25 dbm LO power.

Theoretical values are not shown on the figures but instead are given in Table I in order to compare the MOSFET mixer with a hot-carrier diode double-balanced mixer (Ref. 11).

The difference in conversion loss between the theory and experiment for a MOSFET mixer was explained in Section III-C. This difference is 3 dB greater and is due to odd-order parasitic impedances and impedances reflected through the transformers to the source and drain loops. These impedances will decrease the drain current, thus the output voltage and increase the conversion loss. Some measured conversion loss versus LO power plots are shown in Figure 25, 26, 27 and 28 with 0 dbm RF power in all cases. Maximum IF output was obtained at $f_{RF} = 12$ MHz and $f_{LO} = 42$ MHz with 18 dbm LO power, 4 volts DC gate bias and -1 volt DC substrates bias. The conversion loss is 3 dB.

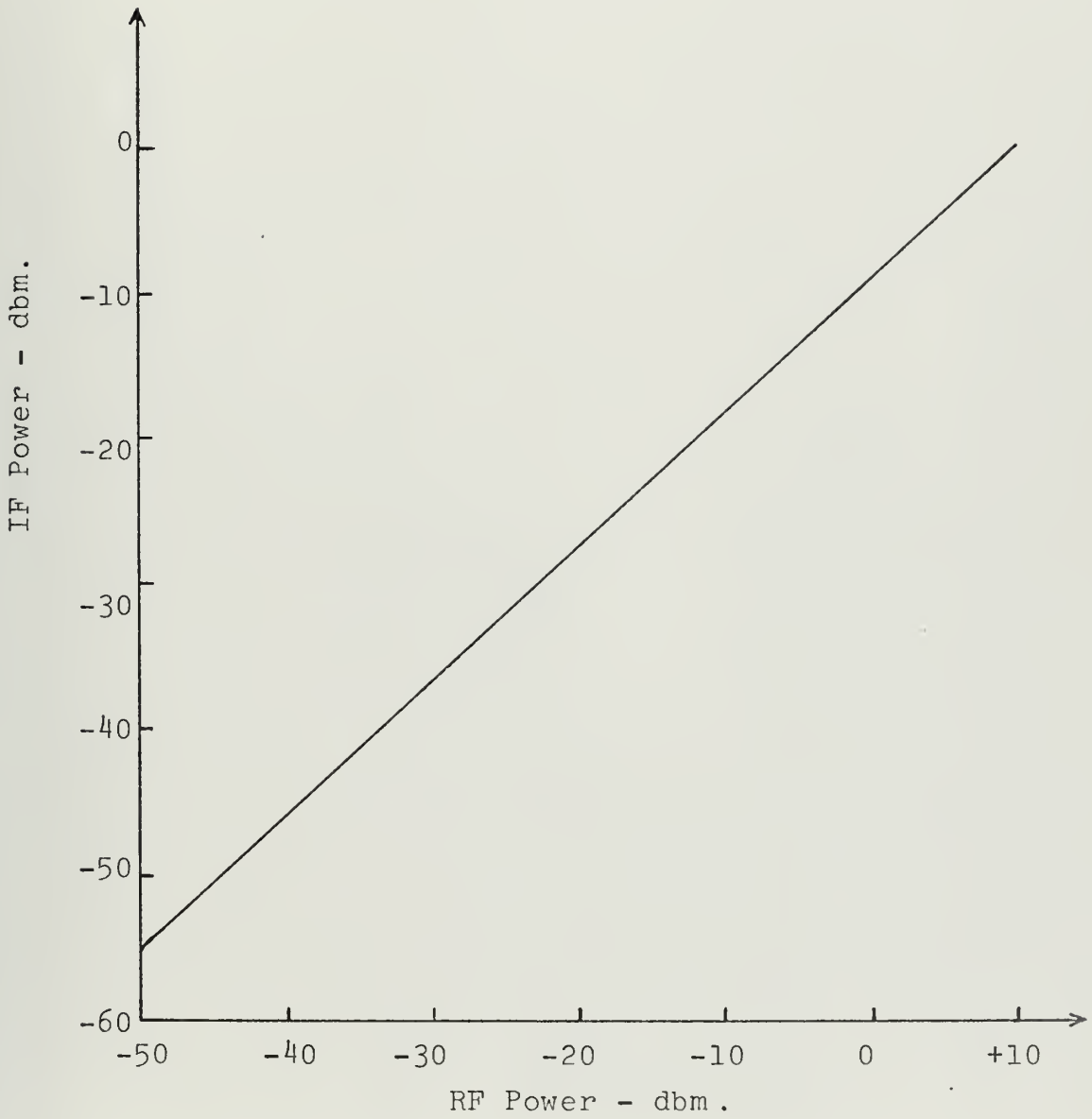


Figure 23. IF Power Versus RF Power for $P_{LO} = 18$ dbm, $f_{RF} = 10-50$ MHz and $f_{LO} = 40-70$ MHz.

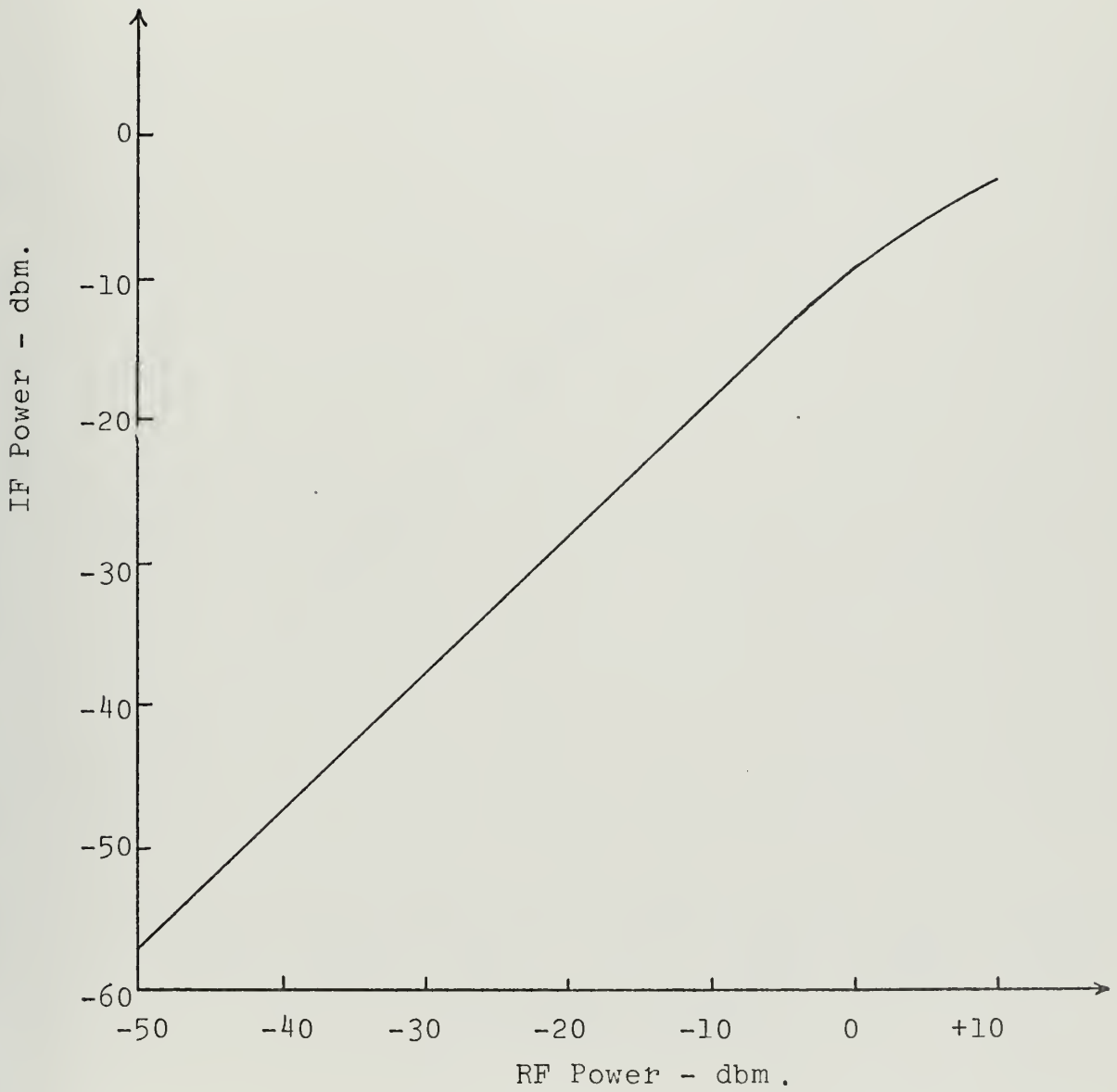


Figure 24. IF Power Versus RF Power for $P_{LO} = 25$ dbm, $f_{RF} = 75-150$ MHz and $f_{LO} = 105-180$ MHz.

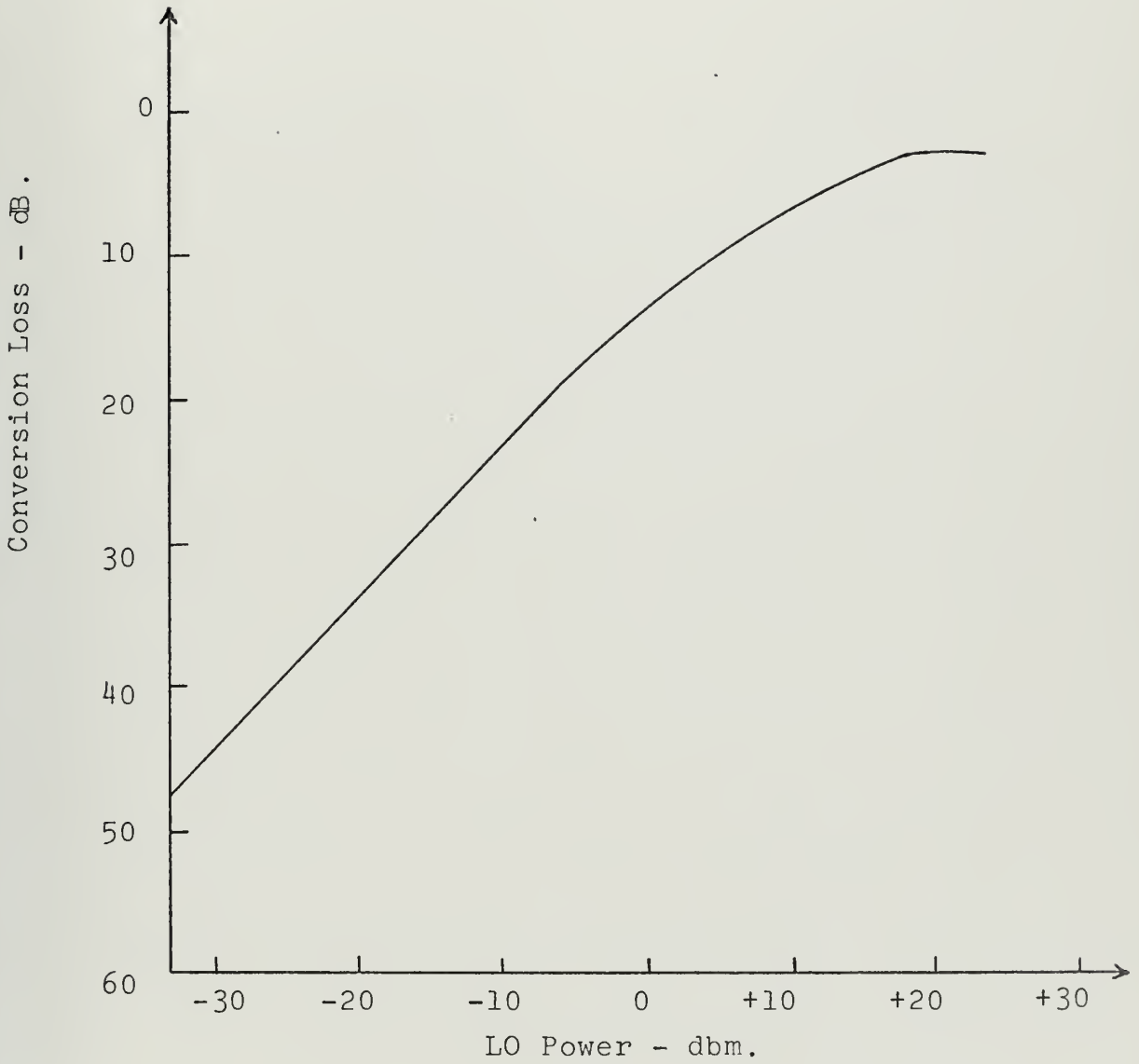


Figure 25. Conversion Loss Versus LO Power for $P_{RF} = 0$ dbm, $f_{RF} = 12$ MHz and $f_{LO} = 42$ MHz.

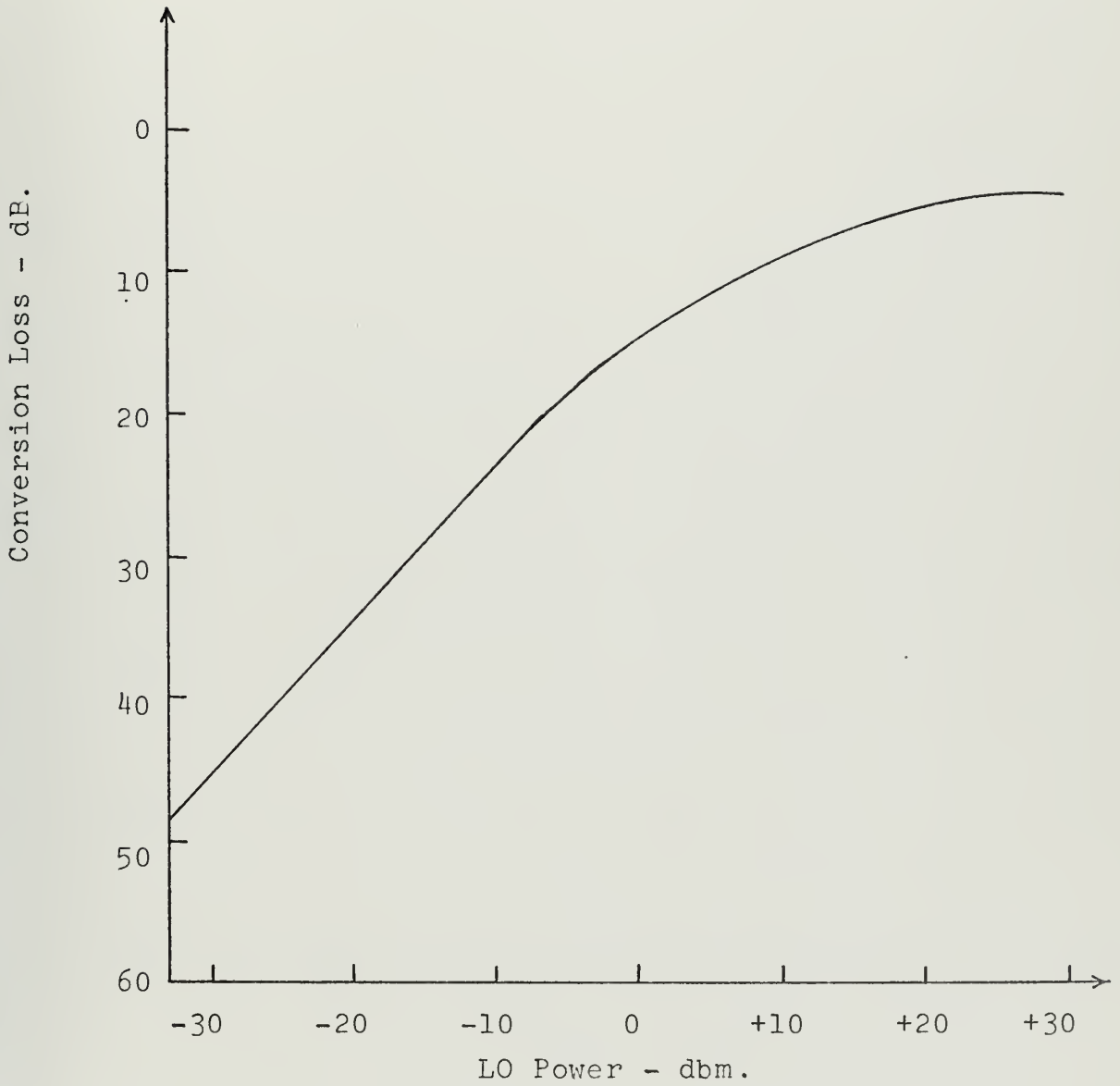


Figure 26. Conversion Loss Versus LO Power for $P_{RF} = 0$ dbm, $f_{RF} = 23$ MHz and $f_{LO} = 53$ MHz.

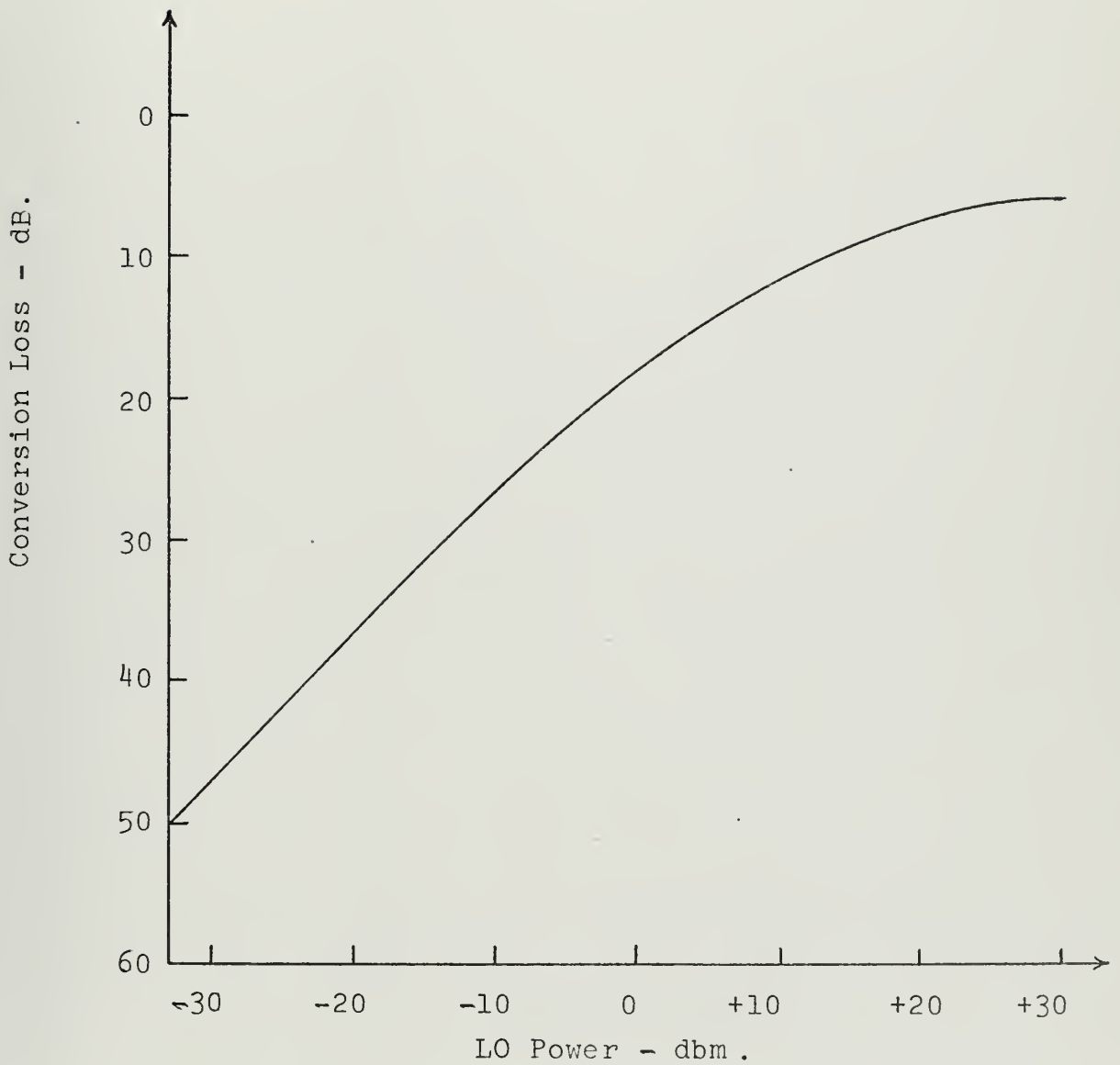


Figure 27. Conversion Loss Versus LO Power for $P_{RF} = 0$ dbm, $f_{RF} = 40$ MHz and $f_{LO} = 70$ MHz.

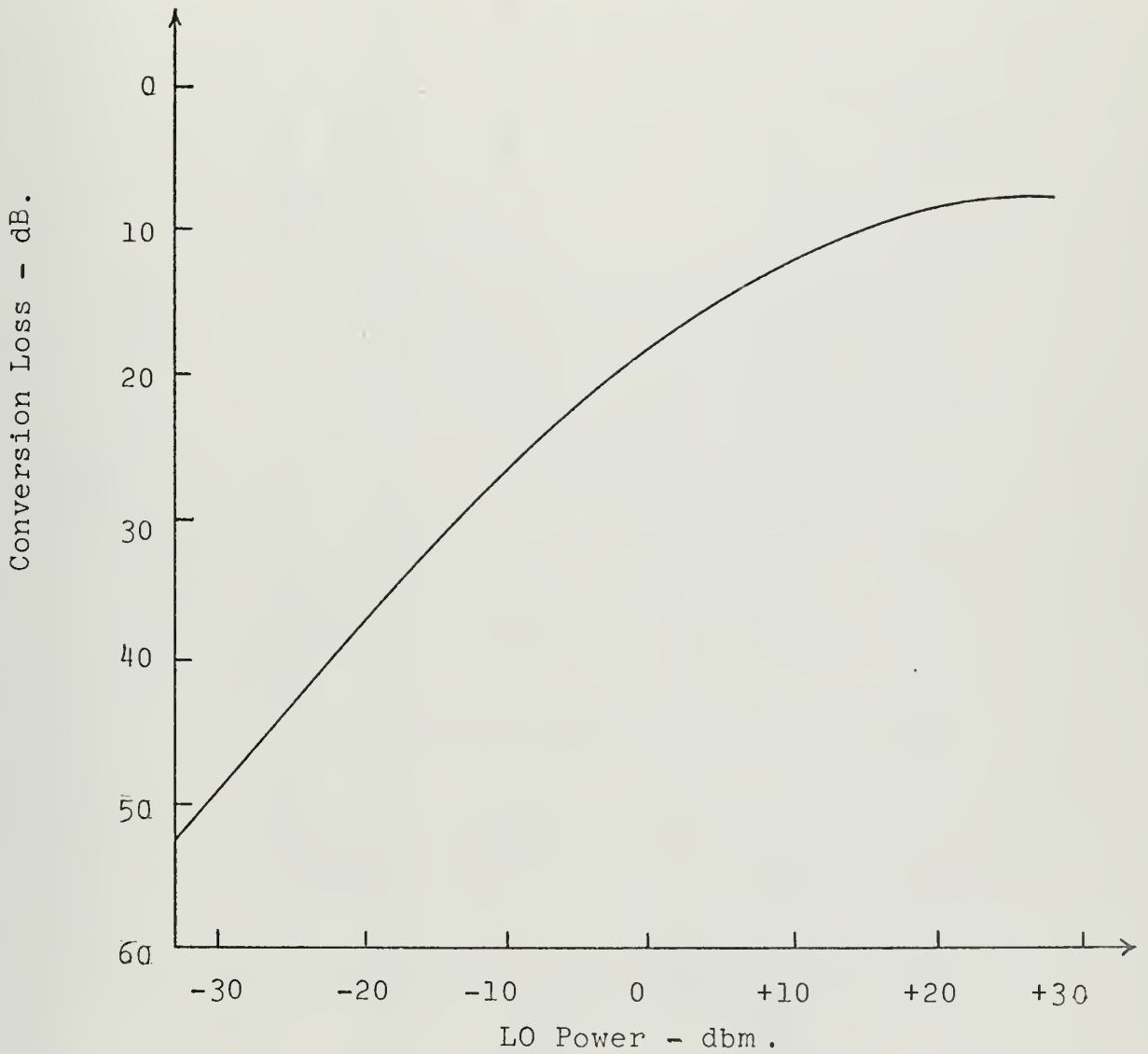


Figure 28. Conversion Loss Versus LO Power for $P_{RF} = 0$ dbm, $f_{RF} = 75$ MHz and $f_{LO} = 105$ MHz.

TABLE I
COMPARISON OF THE MIXERS

Type	Theoretical Conversion Loss	Measured Conversion Loss	Theoretical RF Isolation	Measured RF Isolation	Theoretical LO Isolation	Measured LO Isolation
Hot-Carrier Diode Double-Balanced Mixer	7.4 dB	9 dB	perfect	36 dB	perfect	42 dB
Balanced-bridge Switching-state MOSFET Mixer	0	3 dB	perfect	47 dB	perfect	60 dB

As indicated in Table I, theoretical RF and LO isolations do not agree with the experiment. Disagreement is attributed to the parasitic and reflected impedances, impedance mismatching, transformer losses and circuit-board design effects. Perfect isolation is not achieved due to the coupling effect of stray capacitances between the input and output ports.

In the theoretical analysis it is shown that the output voltage depends on the LO voltage. Therefore, conversion loss depends upon the LO drive level--the higher the LO voltage the lower the conversion loss (below the point where compression begins), that is demonstrated in Figure 25, 26, 27 and 28 by the measured values of conversion loss versus LO power. Lower conversion loss also results in a wider dynamic range. Theory shows spurious responses due to the even harmonics of both RF and LO signals are eliminated and IM responses due to the even harmonics of the LO signals are also suppressed. Both odd-order impedances at the input and output contribute to the generation of third-order IM response.

Table I also shows that the MOSFET mixer is superior to a hot-carrier diode double-balanced mixer in conversion loss, RF and LO isolation.

IV. CONCLUSIONS AND RECOMMENDATIONS

As mentioned in the Introduction, mixer design becomes extremely important in high level signal environment and high frequency applications in establishing receiver performance. Therefore, there is a need to design mixers with the widest possible dynamic range, low conversion loss, and minimum IM distortion and other spurious responses. In terms of IM, the third-order IM distortion in mixers is a very important factor in determining the mixer's dynamic range. This distortion should be predictable from theoretical considerations if its generation is to be understood and if high dynamic range receivers are to be designed.

In this study a theory for conversion loss and IM distortion in a broadband balanced-bridge switching-state MOSFET mixer has been derived using the two-state ideal case mixer assumption to identify the sources of conversion loss and IM generation. The conversion loss was compared with the experimental determination. The theory was given in the presence of an interfering signal and it was shown that CM, IM and spurious responses can be reduced. It was also indicated that the conversion loss in MOSFET mixer is improved 7.4 dB compared to hot-carrier diode double-balanced mixer, and RF and LO isolations were found to be perfect. It was also found that over a certain range of gate bias and substrate bias voltages the conversion loss

was quite close to the theoretical predictions. Below this bias range transition region IM distortion became significant and above this range FET heating effects produced a change in the FET's "ON" resistances, which caused the conversion loss and IM to depart from theory, since an ideal case was assumed.

Close agreement with the theory and experiment was found for conversion loss with 3 dB discrepancy. The most likely explanation for this discrepancy appears to be odd-order parasitic and reflected impedances, impedance mismatching and circuit-board design effect. RF and LO isolations disagreement with the theory and experiment was found to be greater. The explanation indicated stray capacitances, transformer losses, and unbalance in the circuit. An increase in frequency decreased both RF and LO isolations and indicated that effect of stray capacitances. Experiment also shows that the symmetry of the circuit-board design and choice of the core material affects the performance in terms of conversion loss and isolations.

Through both theoretical and experimental work it has been shown that the MOSFET mixer enjoys a better conversion loss which implies wider dynamic range together with RF and LO isolation and minimum number of spurious and IM responses, compared to the hot-carrier diode double-balanced mixer.

Several conclusions may be drawn from these results. First, it may be stated that third-order IM distortion sources in MOSFETs are understood and that, over a range of

bias levels, only the sources used in the two-state assumption are significant and are predictable. Second, a square-wave LO drive might result significant reduction in the IM. Third, an optimum source impedance might exist for a minimum third-order IM in the mixer, which depends on the LO drive level in a way that is predictable from theory over a range of LO drive levels.

Further study should be undertaken to examine IM distortion in MOSFET mixer. In order to resolve the possible discrepancy between theory and practice in mixer IM, much experimentation should be done to study the transition region IM. Square wave generators with shorter rise times may be constructed to see if this discrepancy is attributed to transition region IM. Other types of IM distortion, principally second order, should be investigated both theoretically and experimentally. It is also worthwhile to look for possible improvements in dynamic range through more complete mixer and device characterization.

Since the measuring equipment used in this study severely limited the experimental evaluations, meaningful measurements can only be made by using very "clean" signal generators with high output power and a high performance spectrum analyzer, neither of which are currently available commercially.

APPENDIX A

NONLINEAR RESISTANCE MIXER

1. Frequency Conversion and Mixer Operation

The characteristics of a nonlinear device in which the transfer function is a function of the values of one of the input variables may be represented as a power series expanded around some point value. We may define the value of a nonlinear resistor as a power series in current, I , the instantaneous current through the resistor:

$$R(I) = R_0 + R_1 I + R_2 I^2 + R_3 I^3 + \dots + R_n I^n . \quad (A-1)$$

Then the voltage across the resistor shown in Figure A-1 is:

$$V = IR(I) = R_0 I + R_1 I^2 + R_2 I^3 + R_3 I^4 + \dots + R_n I^{n+1} . \quad (A-2)$$

Assume the series can be terminated with little error at the second term such that:

$$V = R_0 I + R_1 I^2 . \quad (A-3)$$

Suppose the current consists of two sinusoidal currents, I_1 and I_2 , at frequencies f_1 and f_2 . Then the current through the resistor is,

$$I = I_1 + I_2 = I_1 \cos \omega_1 t + I_2 \cos \omega_2 t . \quad (A-4)$$

The output voltage becomes,

$$V = R_0 (I_1 \cos \omega_1 t + I_2 \cos \omega_2 t) + R_1 (I_1 \cos \omega_1 t + I_2 \cos \omega_2 t)^2 \quad (A-5)$$

where $R_0 (I_1 \cos \omega_1 t + I_2 \cos \omega_2 t)$ is the linear term which simply

reproduces the input signal. However, the square term $R_1(I_1 \cos \omega_1 t + I_2 \cos \omega_2 t)^2$ gives:

$$V_{sq.} = R_1(I_1^2 \cos^2 \omega_1 t + 2I_1 I_2 \cos \omega_1 t \cos \omega_2 t + I_2^2 \cos^2 \omega_2 t). \quad (A-6)$$

Recalling and using some trigonometric identities $\cos^2 x = (1/2)(1 + \cos 2x)$ and $\cos x \cos y = (1/2)[\cos(x+y) + \cos(x-y)]$, equation (A-6) becomes:

$$V_{sq.} = R_1 \left[\frac{1}{2}(I_1^2 + I_2^2) + \frac{1}{2}I_1^2 \cos 2\omega_1 t + \frac{1}{2}I_2^2 \cos 2\omega_2 t + I_1 I_2 \cos(\omega_1 + \omega_2)t + I_1 I_2 \cos(\omega_1 - \omega_2)t \right]. \quad (A-7)$$

It is clear that the $V_{sq.}$ term gives output signals at the frequencies DC, $2f_1$ and $2f_2$, $f_1 + f_2$ and $f_1 - f_2$.

If we define f_1 as the LO frequency and f_2 as the RF frequency, $f_{IF} = \pm(f_1 - f_2)$; the square-law nonlinear resistance can be used as a frequency converter or the simplest mixer. This converter will also respond to a signal at the image frequency, f_i , chosen such that $f_i = f_{LO} + f_{IF}$. A

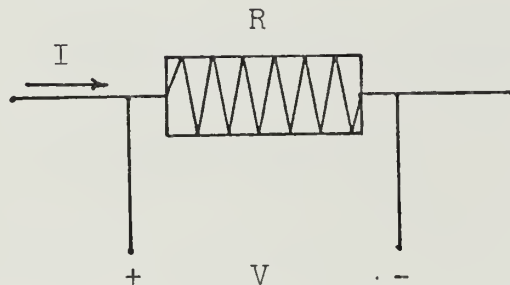


Figure A-1. Nonlinear Resistance Mixer.

signal at f_i frequency will combine with the LO signal to produce output frequencies of the form $\pm f_i \pm f_{LO}$, and the difference product is also equal to the IF frequency. For the purposes of this discussion, it is assumed that the image response is eliminated through some unspecified means.

2. Intermodulation Distortion

At the output port of this mixer,

$$V_{IF} = R_1 I_{RF} I_{LO} \cos \omega_{IF} t . \quad (A-8)$$

The assumption has been made that the resistance can be described adequately by a linear term and a square-law term. In practice this is not valid over an infinite range, and at some lower level the cubic term of the power series expansion begins to contribute measurable output power:

$$V_{cubic} = R_2 (I_1 \cos \omega_1 t + I_2 \cos \omega_2 t)^3 . \quad (A-9)$$

The cubic term, when expanded, becomes:

$$\begin{aligned} V_{cubic} = R_2 & \left[\left(\frac{3}{4} I_1^3 + \frac{3}{2} I_1 I_2^2 \right) \cos \omega_1 t + \left(\frac{3}{4} I_2^3 + \frac{3}{2} I_1^2 I_2 \right) \cos \omega_2 t \right. \\ & + \frac{1}{4} I_1^3 \cos 3\omega_1 t + \frac{1}{4} I_2^3 \cos 3\omega_2 t + \frac{3}{4} I_1^2 I_2 \cos(2\omega_1 + \omega_2) t \\ & + \frac{3}{4} I_1^2 I_2 \cos(2\omega_1 - \omega_2) t + \frac{3}{4} I_1 I_2^2 \cos(2\omega_2 + \omega_1) t \\ & \left. + \frac{3}{4} I_1 I_2^2 \cos(2\omega_2 - \omega_1) t \right] \quad (A-10) \end{aligned}$$

and contains frequency components at f_1 and f_2 , at $3f_1$ and $3f_2$ and at $2f_1 \pm f_2$ and $2f_2 \pm f_1$. These terms at frequencies of the form $2f_m \pm f_n$ are the third-order IM terms, spurious responses generated by the mixer at an output frequency

different from the input frequencies. The danger occurs when one of the third-order sums or differences falls near the desired signal; in this case the receiver will amplify, demodulate, and will deliver this internally generated spurious signal to the output as if it were present at the input.

The actual mechanism for generation of third-order IM is a bit more complex than appears from the foregoing discussion. However, a brief discussion can indicate the process of IM generation:

Assume the input port sees the LO at f_{LO} , and two undesired signals at f_1 and f_2 . Further assume that the desired signal is at an frequency $f_{RF} = f_{LO} - f_{IF}$ and that the undesired signals occur such that $2f_1 - f_2 = f_{RF}$. This is the normal situation with third-order IM. The cubic term will produce a voltage at the third-order difference frequency, $2f_1 - f_2$, but this voltage must still be converted down to the IF frequency by the square-law portion of the device. In short, any IM production mechanisms must occur separately from the conversion mechanism, any third-order IM is generated by signals going through the mixer twice--once to generate the odd-order term, and once to convert to odd-order term to the IF frequency.

To illustrate this, let the resistance power series expansion be divided into odd and even functions of current (I) through resistance:

$$R(I) = R_o(I) + R_e(I) , \quad (A-11)$$

then, the current is common to both the odd and even parts of the resistance, and the voltage may be divided into odd and even functions:

$$V = V_o + V_e \quad (A-12)$$

where $V_o = IR_e(I)$ and $V_e = IR_o(I)$; the cubic term shows up in V_o :

$$V_{\text{cubic}} = \frac{3}{4} R_2 I_1^2 I_2 \cos(2\omega_1 - \omega_2)t \quad (A-13)$$

This is transmitted through the external networks as an odd-order current into the even-order resistance terms; if we let the transmission constant be K , then the final IM voltage is

$$V_{\text{IM}} = \frac{3}{4} K R_1 R_2 I_1^2 I_2 I_{\text{LO}} \cos \omega_{\text{IF}} t \quad (A-14)$$

It is assumed that both the signal power that is converted to the IF, and the IM power that is also at IF, have the same load since they are at the same frequency.

3. The Dynamic Range

The dynamic range (D.R.), defined as the range between some arbitrary signal power and the lower IM signal power is,

$$\text{D.R.} = \frac{P_{\text{generated by signal}}}{P_{\text{generated by IM signal}}} \quad (A-15)$$

Then,

$$\text{D.R.} = \frac{|V_{\text{IF(signal)}}|^2}{|V_{\text{IF(IM signal)}}|^2} = \frac{|R_1 I_{\text{RF}} I_{\text{LO}}|^2}{\left| \frac{3}{4} K R_1 R_2 I_1^2 I_2 I_{\text{LO}} \right|^2} \quad (A-16)$$

This measure of dynamic range may be related to the usual measurement by setting IM power level at 10 dB above the noise level. Then the output signal will be greater than the IM power by the amount of the dynamic range in dB.

Assume equal signal power and undesired signal powers such that:

$$I_{RF} = I_1 = I_2 = I;$$

then,

$$D.R. = \frac{1}{\frac{9}{16} K^2 R_1^2 I^4} \cdot \quad (A-17)$$

(Note that since R_1 has units of volts/amps² and R_2 has units of volts/amps³, the K has units of amps/volt and the dynamic range is dimensionless, as expected.)

Examining the above expression for dynamic range, it becomes clear that IM may be reduced and D.R. increased by lowering the coefficient of the cubic term, as expected, and by reducing the coupling coefficient that allows the third-order terms to feed into the even-order (square-law) frequency conversion portion.

4. Summary of Theoretical Analysis of Nonlinear Resistance Mixer

An interesting feature of this mixer is that without the square-law conversion term, no IM will be generated. If some way were found to generate second-order sums and differences without a square-law term the mixer would have an indefinite dynamic range. More properly, if a mixer could be developed with no even-order terms, no IM could be

generated. The pure square-law mixer is normally considered to have this characteristic, but this is not necessarily true, depending on the terminations of the second-harmonic components. If a mixer having a purely cube-law characteristic is fed with the signal and LO frequencies and a DC offset voltage ($f_{DC} = 0$) the output will produce frequencies of the form $\cos(\omega_{LO} \pm \omega_{RF})t = \cos\omega_{IF}t$ and frequency conversion will take place. The limitation is that all higher order terms in the polynomial expansion will produce IM, both the odd-order terms and even-order terms.

BIBLIOGRAPHY

1. Chirlian, P.M., Electronic Circuits: Physical Principles, Analysis, and Design, p. 184-208, McGraw-Hill Book Co., Inc., 1971.
2. Cobbold, R.S.C., Theory and Applications of Field-Effect Transistors, p. 415-478, Wiley-Interscience, 1970.
3. Gray, P.E., and Searle, C.L., Electronic Principles Physics, Models, and Circuits, p. 313-341, Wiley, 1969.
4. Kwok, S.P., "Field Effect Transistor RF Mixer Design Techniques," WESCON Technical Papers, Vol. 11, Session 8/1, p. 1-9, August 1967.
5. Ernst, R.L., Torriano, P., Pan, W. Y., and Morris, M.M., "Designing Microwave Mixers for Increased Dynamic Range," IEEE Transactions on Electromagnetic Compatibility, Vol. EMC-11, No. 4, p. 130-138, November 1969.
6. Fischer, R., "An Engineer's Ham-Band Receiver," QST, Vol. 54, No. 3, p. 11, March 1970.
7. Ress, W., "Broadband Double Balanced Modulator," Ham Radio, Vol. 3, No. 3, p. 8-17, March 1970.
8. Orloff, L.M., "Intermodulation Analysis of Crystal Mixers," Proceedings of the IEEE, Vol. 52, No. 2, p. 173-179, February 1964.
9. Tucker, D.G., "Intermodulation Distortion in Rectifier Modulators," Wireless Engineer, Vol. 31, No. 6, p. 145-152, June 1954.
10. Belevitch, V., "Linear Theory of Bridge and Ring Modulator Circuits," Electrical Communication, Vol. 25, No. 1, p. 62-73, March 1948.
11. Güler, E., "A Study of Broadband Hot-carrier Diode Mixers," M.S. Thesis, Naval Postgraduate School, Monterey, 1970.
12. Ward, M.J., "A Wide Dynamic Range Single-sideband Receiver," M.S. Thesis, Massachusetts Institute of Technology, Cambridge, 1967.
13. Snyder, R.E., "Intermodulation Distortion in a Broadband Balanced Mixer," M.S. Thesis, Massachusetts Institute of Technology, Cambridge, 1969.

INITIAL DISTRIBUTION LIST

	No. Copies
1. Defense Documentation Center Cameron Station Alexandria, Virginia 22314	2
2. Library, Code 0212 Naval Postgraduate School Monterey, California 93940	2
3. Professor R. W. Adler, Code 52AB Department of Electrical Engineering Naval Postgraduate School Monterey, California 93940	2
4. Lt. (jg) Mustafa Yenigün, Turkish Navy Esref Efendi Sok. No. 197/3 Kurtulus, Istanbul Turkey	2
5. Istanbul Teknik Universitesi Elektrik Fakultesi Taskisla, Istanbul Turkey	1
6. Orta-Dogu Teknik Universitesi Elektrik Fakultesi Ankara, Turkey	1
7. Karadeniz Teknik Universitesi Elektrik Fakultesi Trabzon, Turkey	1
8. Deniz Kuvvetleri Komutanligi Personel Egitim Sb. Mudurlugu Ankara, Turkey	1
9. Deniz Harb Okulu Komutanligi Keybeliada, Istanbul Turkey	1
10. Deniz Makine Sinif Okullari Komutanligi Derince, Kocaeli Turkey	1

DOCUMENT CONTROL DATA - R & D

(Security classification of title, body of abstract and indexing annotation must be entered when the overall report is classified)

1. ORIGINATING ACTIVITY (Corporate author)		2a. REPORT SECURITY CLASSIFICATION	
Naval Postgraduate School Monterey, California 93940		Unclassified	
		2b. GROUP	
3. REPORT TITLE			
A STUDY OF A BROADBAND BALANCED-BRIDGE SWITCHING-STATE MOSFET MIXER			
4. DESCRIPTIVE NOTES (Type of report and, inclusive dates)			
Master's Thesis; December 1971			
5. AUTHOR(S) (First name, middle initial, last name)			
Mustafa Yenigün, Lieutenant (junior grade), Turkish Navy			
6. REPORT DATE		7a. TOTAL NO. OF PAGES	7b. NO. OF REFS
December 1971		77	13
8a. CONTRACT OR GRANT NO.		9a. ORIGINATOR'S REPORT NUMBER(S)	
b. PROJECT NO.			
c.		9b. OTHER REPORT NO(S) (Any other numbers that may be assigned this report)	
d.			
10. DISTRIBUTION STATEMENT			
Approved for public release; distribution unlimited.			
11. SUPPLEMENTARY NOTES		12. SPONSORING MILITARY ACTIVITY	
		Naval Postgraduate School Monterey, California 93940	
13. ABSTRACT			
<p>A theory for a mixer using four MOSFETs in a broadband balanced-bridge configuration has been developed in terms of both ideal models and approximate representations for departures from the ideal case. An interfering signal is assumed to be present in order to analyze intermodulation and cross-modulation distortions.</p> <p>The mathematics of a MOSFET mixer are developed and compared with the conversion properties and intermodulation limitations of the simple nonlinear-resistance mixer.</p> <p>Measurements are made in the 10-200 MHz range and close agreement with the theory is found for conversion loss. Disagreement in RF and LO isolations is attributed to stray capacitances and impedance mismatching. It is also shown that circuit-board and transformer design greatly affects performance of a mixer.</p> <p>A comparison of MOSFET and hot-carrier diode double balanced mixers is given and it is indicated that the MOSFET mixer is superior in conversion loss and RF and LO isolations.</p>			

KEY WORDS	LINK A		LINK B		LINK C	
	ROLE	WT	ROLE	WT	ROLE	WT
Mixing Circuits						
Crystal Mixers						
MOSFETs						

Thesis

Y36

c.1

Yeniğün

A study of a broadband
balanced-bridge switch-
ing-state MOSFET mixer.

135539

Thesis

Y36

c.1

Yeniğün

A study of a broadband
balanced-bridge switch-
ing-state MOSFET mixer.

135539

thesY36

A study of a broadband balanced-bridge s



3 2768 000 98829 9

DUDLEY KNOX LIBRARY